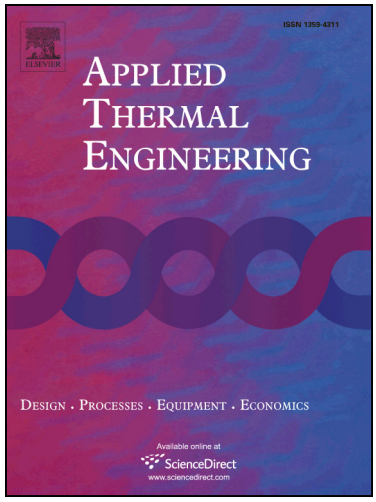

Research paper

Heat transferred to the workpiece based on temperature measurements by IR technique in dry and lubricated drilling of Inconel 718

M. Cuesta, P. Aristimuño, A. Garay, P.J. Arrazola

PII: S1359-4311(16)30693-7
DOI: http://dx.doi.org/10.1016/j.applthermaleng.2016.05.040
Reference: ATE 8253

To appear in: *Applied Thermal Engineering*

Received Date: 11 September 2015
Revised Date: 3 February 2016
Accepted Date: 3 May 2016

Please cite this article as: M. Cuesta, P. Aristimuño, A. Garay, P.J. Arrazola, Heat transferred to the workpiece based on temperature measurements by IR technique in dry and lubricated drilling of Inconel 718, *Applied Thermal Engineering* (2016), doi: http://dx.doi.org/10.1016/j.applthermaleng.2016.05.040

Applied Thermal Engineering 00 (2015) 000–000

Available online at www.sciencedirect.com

SciVerse ScienceDirect

Journal homepage: www.journals.elsevier.com/applied-thermal-engineering/

HEAT TRANSFERRED TO THE WORKPIECE BASED ON TEMPERATURE MEASUREMENTS BY IR TECHNIQUE IN DRY AND LUBRICATED DRILLING OF INCONEL 718

M. Cuesta [a] *, P. Aristimuño* [a] *, A. Garay* [a] *, P. J. Arrazola* [a]

[a] *Faculty of Engineering, Mondragon University, Arrasate-Mondragón, Spain*

ARTICLE INFO

Article history:
Received 00 December 00
Received in revised form 00 January 00
Accepted 00 February 00

Keywords:
Heat partition
Infrared thermography
Inconel 718
Temperature
Drilling
Lubricated

ABSTRACT

In manufacturing aeronautical critical components, such as turbine discs commonly made of Inconel 718, surface integrity is crucial to ensure their fatigue life. Among the machining processes used, the drilling operation is one of the most critical as overheating can occur causing thermal damage to the hole. The amount of heat dissipated could determine the nature of deformation in the machining of Inconel 718. Nevertheless no detailed studies have determined experimentally the differences between the fractions of heat transferred to the workpiece (β) for dry and lubricated drilling. In this context, the thermal and mechanical loads (measured by IR technique and a piezoelectric dynamometer) affecting the drilling of Inconel 718 have been studied. Four different cutting conditions both in dry and lubricated conditions were tested. In order to obtain β, the study presents a model based on a new experimental method. The maximum β values were achieved in the unlubricated tests (around 0.20). By contrast, in the lubricated tests β range from 0.065 to 0.078. Therefore the fraction of heat conducted to the workpiece show maximum differences of 72% and minimum of 57% depending on the application or not application of coolant. Additionally, the obtained trends of β relative to Peclet number (that is dependent on the cutting speed, feed and drill diameter) are shown.

1. Introduction

Inconel 718 is one of the most used High Strength Thermal Resistant (HSTR) materials in the manufacturing of critical parts of aircraft engines such as turbine discs due to its high strength/weight ratio operating at extreme pressure and temperatures. However it is difficult to machine due to the inherent characteristics of the material such as the work hardening generated in the machining process, the low thermal conductivity or carbides presence [1, 3, 4]. Tool wear condition has a remarkable influence on Surface Integrity (SI), e.g., residual stresses, undesirable alteration of machined surfaces or induced strain loadings on the sub-surface, which in turn affect fatigue life of a component [5, 6]. For instance, it has been observed that different types of defects appeared on the machined component depending on whether the machining surface is affected mechanically, thermally or chemically [7]. Heat affected layers (phase transformation, cracking, white layer…) reduced greatly the fatigue performance of the machined parts. Furthermore the combination of high temperatures and high pressures induced high stresses that generate microstructural changes. It has been observed that while thermal dominant machining deformation induced tensile residual stresses in the machined surface, the mechanically dominant machining deformation induced compressive residual stresses [7, 8]. This effect might be in relationship with the amount of heat dissipation that determines the nature of deformation in the machining of Inconel 718 [9].

* *Corresponding author.* Tel.: +34-943-739-682 ; fax: +0-000-000-0000.
E-mail address: mcuesta@mondragon.edu (M. Cuesta)

xxxx-xxxx/$ – see front matter © 2015 Elsevier ltd. All rights reserved.
doi: xxxxxxxxxxxx

It should be highlighted that the majority of studies into the influences on surface integrity have focused on turning or milling [2, 6, 8, 9, 10]. The drilling process has largely been overlooked [11]. This is a surprising fact, as the holes are critical features with reference to fatigue performance [7]. This criticality is determined by two aspects; (i) the holes are critical geometrical features of the turbine discs and (ii) the drilling process itself. Due to its geometry, the holes are areas with high stress concentrations where the maximum stress values could be achieved. In that sense, it is important to prevent the thermal damage that could be caused by the overheating during the drilling due to an inadequate chip removal and the lack of lubrication. It is for these reasons that critical machined parts require a validation process to ensure the quality of the pieces in fatigue life. This validation generally involves freezing the cutting conditions by checking metallurgical analysis and fatigue tests to ensure that the cutting conditions are "safe". This process is complicated and involves high costs. Therefore, correlations between the cutting conditions and surface integrity would help to optimize manufacturing these components [12]. It is at this point that the monitoring and modelling of machining HSTR alloys plays a decisive role to solve problems related with the thermal loads [13].

Energetic balance distributions for machining processes have been studied since the 50's. Most of the models are based on the same physical laws and use the same hypothesis, usually with the main objective to determine the amount of heat transferred to the workpiece. Stephenson analyses different energetic balance models [14] and states that, Loewen and Shaw's heat distribution model [15] shows the best performance. This model treated the workpiece as a semi-infinite body subject to a heat flux imposed by a moving source of constant flux. It analyzes the 2D orthogonal cutting process based on Jaeger's frictional theory of the moving sources of sliding contacts [16] and Blok's principle of heat distribution [17].

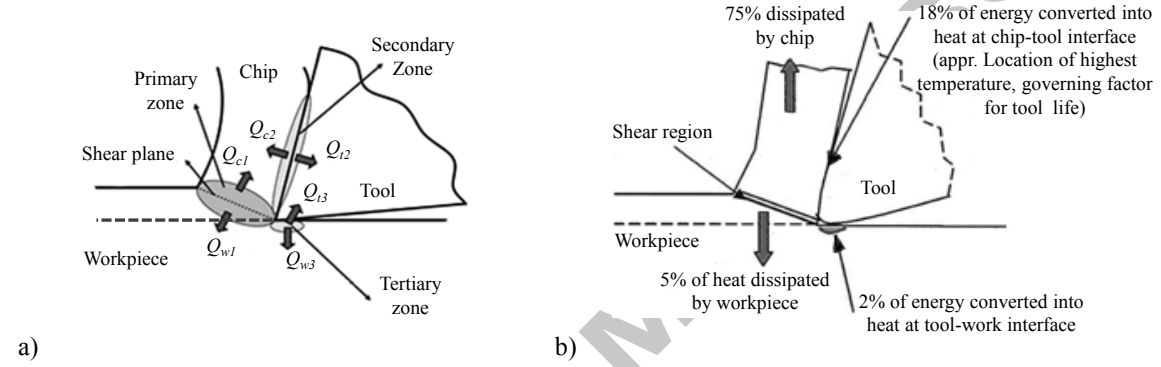

Fig. 1 – (a) Heat generation zones in cutting process (b) Typical energy distribution model in metal cutting at conventional speed [24].

Looking to the drilling process, thermal aspects have long been investigated from an analytical point of view [18, 19]. These studies are based on 2D orthogonal cutting theory and showed a general overview of the chip formation when drilling. Many of this researchers focused on evaluating and predicting the generation and flow of heat into the tool, the chips and the workpiece [20, 21, 22]. As it is shown in Fig.1 (a), the cutting heat is generated at three different deformation regions. Each zone has its own singularities, so the amount of heat that flows from each zone is different. In Fig. 1 (b) an example of heat dissipation in metal cutting is illustrated where approximately 25 % of energy from machining converts into heat. With this assumption, machining performance can be affected by the high thermal gradients. Temperature in primary deformation zone influences the mechanical properties of the workpiece. Whilst temperature at the secondary deformation zone strongly affects tool life [23], most of the heat generated in the tool-chip contact zone flows to the tool (around 18% of total heat [24]). This partial heat conducted to the tool leads to the tool temperature rise and the remaining heat is taken away by the fixed tool holder and the air [22]. Concerning to the workpiece, the transmitted cutting heat comes from the shear deformation zone. In Bonos advection heat partition model for drilling [20], all the heat generated on the shear plane is conducted directly into the workpiece. Thus, the heat generated by shearing is applied as a heat flux into the material below the cutting edge. This confirms that, as the drill moves into the workpiece, heat is continually added to the material so temperatures rarely reach a steady state and increase with the hole depth. Moreover, most of the models predict temperatures focus on the primary cutting edges, but other heat sources, such as friction between drill flutes and the workpiece or the influence of the chisel edge, should be taken into account.

The influence of temperature is more significant when machining HSTR alloys due to their heat resistance and poor thermal conductivity. Such thermal behavior must also be considered for understanding the distribution of residual stresses as high temperatures are well known to induce tensile stresses on the workpiece surface [7]. Rech et al. [25], tested on a special tribometer several materials including the Inconel 718. They employed different lubrication conditions and presented results and models for the portion of heat flux transmitted to the tool. Research works as this, give valuable information, but when the objective is to study the surface integrity and understand the influence of the different machining parameters, the focus should be put on the workpiece. In that line, Soriano et al. [21] studied the heat flow into the workpiece from the experimentally obtained workpiece temperatures (by IR technique) and cutting forces when dry drilling bovine cortical bone. The authors showed how the heat fractions decrease as the Peclet number increase. They conclude that this is a physically feasible result and supports the view of a critical Peclet number below which increasing cutting speed and feed lead to increasing temperatures in the workpiece and above which temperatures reduce. The Peclet number (frequently used in heat transfer theory) is widely used for thermal study of machining process. The heat transferred to the workpiece is controlled by Peclet number and the larger it is, the less heat escapes and the more is convected into the chip [26]. Related to this, Fleischer et al. showed an increase of the heat flux mainly caused by reducing the feed per tooth, ie. the undeformed chip thickness, when dry drilling of power train castings [27]. Segurajauregui and Arrazola [28] used the inverse simulation technique to calculate the heat input to the workpiece when drilling aluminium with MQL. They determined that an increase of the cutting speed and feed

rate leads to a decrease in heat input and temperature. Biermann and Iovkov [29] also concluded that the heat input to the workpiece could be significantly reduced increasing the feed values when deep hole drilling aluminium cast alloy applying MQL. Furthermore, the strong dependence of the heat flux and the heat partition to the workpiece on the undeformed chip thickness observed by Fleischer et al., was also detected when dry milling of steel [30].

Davies et al. in their review work stated that different methods such as thermocouples and infrared measurements have been used to study the temperatures in the drilling process [31]. Brinksmeier et al. [32] measured the process temperature when drilling Ti6Al4V with an infrared camera and showed a direct correlation between the process temperatures and the chip extraction at different conditions. With low chip extraction the chip accumulation caused a surface smoothening due to the interaction between the chip and the minor cutting edges. These conditions caused the increase in the cutting forces and temperatures due to intensive plastic deformation and friction. Focusing on the HSTR alloys, Kwong et al. [33] conducted a study of tool temperature drilling in severe conditions (VB=0, V_c=25m/min, f=0.10 rev/mm, dry) of the RR1000 HSTR alloy. They used the method of thermocouple inserted through the internal cooling of the drill. They measured temperatures of 750 ºC. In that line, temperatures between 500-650ºC have been reported during drilling of Inconel 718 under severe conditions (VB=0.3, V_c=35m/min, f=0.12 and 0.05 rev/mm, dry) [34, 35]. Also temperature distribution of the numerical simulations carried out for Alloy 718, Waspalloy, Alloy 720Li and RR100 nickel-base superalloys showed maximum temperatures of 700ºC at the tool/workpiece interface [36]. As it can be seen, the majority of the studies analyzing temperature during the drilling of HSTR alloys have been focused on severe machining conditions (high material removal rates in dry cutting conditions). In addition, the temperatures analyzed usually correspond to the tool temperature. There have been no detailed investigations which obtained experimentally values of the heat transferred to the workpiece for externally lubricated drilling. And focusing on HSTR alloy drilling, no research has been found that studies the heat transferred to the workpiece. It is therefore interesting to deepen the study of the heat transferred to the workpiece while drilling dry and lubricated HSTR alloys.

The non-accepted thermally abused layers and the so called “white layers” can appear due the absence of coolant with or without and excessive tool wear [36]. Industrial surface quality standards specify that severe plastic deformations and/or thermally abused layers are not accepted on the Inconel 718 part surfaces drilled. In order to study the differences concerning the heat distribution in different scenarios, in this article, the temperature when drilling Inconel 718 with different cutting conditions in dry and externally lubricated have been studied. For that purpose a new experimental set-up was developed to enable the analysis of lubricated holes. To measure the workpiece temperature an infrared thermography (IR) camera was used. Thermography (thermal imaging) is a well-established experimental method for studying cutting tool [37] and workpiece [21] temperature distributions. The developed set-up enables to study the dry and lubricated drilling processes so the study of 4 different cutting conditions in dry and externally lubricated situations was done. Finally, the heat transferred to the workpiece for the tested different conditions was calculated.

Nomenclature

c	Specific heat (J/kg·K)
d_1	Generated hole diameter (mm)
d_2	Diameter of the heated cylinder (mm)
d_{drill}	Drill diameter (mm)
f	Feed per revolution (mm/rev)
f_z	Feed per tooth (mm/tooth)
F_z	Feed force (N)
F_{cut}	Cutting force (N)
h	Distance between the drilled hole and the infrared filming surface (mm)
K_s	Specific cutting force (N/mm^2)
L	Drilled depth (mm)
M_z	Torque (N.m)
Pe	Peclet number ( )
Q_{in}	Heat in introduced due to drilling process (J)
Q_c	Heat in the chip (J)
Q_t	Heat in the tool (J)
Q_w	Heat in the workpiece (J)
R_1	Fraction of heat generated on the shear plane conducted into the chip ( )
S_c	Cross section area of work material (mm^2)
t_{cut}	Cutting time (s)
t_1	Uncut chip thickness (mm)
V_f	Feed rate (mm/s)
V_c	Cutting speed (m/min)
VB	Average flank wear (mm)
W	Work done in cutting (J)
z	Teeth number ( )
α	Rake angle (º)
α_w	Workpiece diffusivity (m^2/s)
β	Fraction of generated heat flowing into the workpiece ( )

B_0	Helix angle (º)
γ_{sh}	Shear strain in the primary deformation zone
ΔT	Temperature increment (K)
$2\kappa_t$	Point angle (º)
θ	Clearance angle (º)
ρ	Density (kg/m^3)
ω	Rotational speed of the tool (rev/s)

2. Experimental procedure

2.1. Set-up, Measure Equipment and Methods

In this study, the temperature when drilling Inconel 718 in dry and externally lubricated condition was studied and a new experimental set-up was developed to enable the analysis of lubricated and unlubricated holes. The thermal phenomena of the workpiece were studied, as well as other typical machining parameters such as feed force (F_z) or torque (M_z). Fig. 2 (a) shows a diagram of the employed set-up for the drilling tests and Fig. 2 (b) shows a 3D detail of the analyzed zone. To measure the cutting forces (F_z and M_z), the drilled workpieces were clamped on a Kistler 9272 piezoelectric dynamometer. Test samples were plates machined to obtain perpendicular faces. Then, these samples were fixed on the top of the dynamometer and placed correctly in front of the FLIR Titanium 550 M IR camera 0.1 m away from the focus. The filming area (one of the side surfaces of the plates) can be observed in Fig. 2 (b). The length of this area was 40 mm and the height was delimitated by the depth (6.5 mm) of the test sample.
The objective was to study the thermal phenomena as close as possible to the cutting zone (the inner wall). In that sense, in order to avoid the lubrication to penetrate and disturb the recording wall, preliminary tests were carried out to define a minimum distance (h) between the drilled hole and the infrared filming surface (Fig. 2 (b)). This being so, the temperatures of the workpiece presented in this study were measured at a distance h=0.5 mm. The temperature rise (ΔT) of each test was extracted as the difference between the achieved maximum temperature and the temperature at the test starting moment. For each hole, all the data was extracted from one point where the maximum temperature gradients were achieved. In all the experimental tests presented the IR camera was set with a 12µm integration time and a frame rate of 500 Hz The procedure to obtain the temperature fields with the IR camera was the same described by Soriano et al. [21] and Segurajauregui and Arrazola [28].

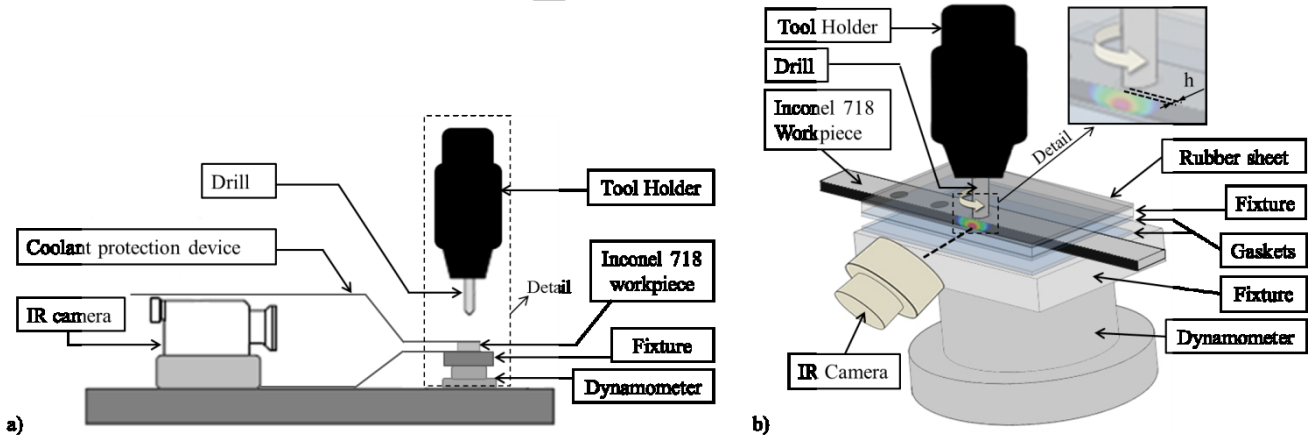

Fig. 2 –Experimental set-up (a) General scheme (b) 3D scheme of the detail in (a).

The signals from the dynamometer (F_z and M_z) were introduced in the analog input module of the machine. As result these signals were visualized and acquired at the same time with a 250 Hz frequency.
As shown in the Fig. 2 (a), a coolant protection device was designed for these tests. The device allowed the use of coolant in the externally lubricated tests, keeping dry the face where the IR camera was recording the heat flux. A detail with the 3D scheme of the solution developed to keep the recording wall dry is shown in Fig. 2 (b). For each test, while the Inconel 718 workpiece was drilled the upper and lower gaskets where also drilled. Thus the oil employed in the lubricated tests enters inside the hole, but did not wet the top of the workpiece and the recording wall.
The set-up was mounted in a vertical CNC milling center and was completed with a Kistler 5019 amplifier and the data analysis software.

2.2. Inconel 718 drilling tests

The workpiece material used for these tests was Inconel 718 rolled annealed and aged (AMS 5596). Each test sample was prepared in an EDM machine to obtain the final rectangular 20mm x 150 mm workpieces. Table 1 shows the chemical composition of the workpieces.

Table 1 – Chemical composition of the employed Inconel 718.

18.63% Cr	17.66% Fe	4.94% Nb	2.89% Mo	0.92% Ti
0.59% Al	0.24% Co	0.13% Si	0.12% Cu	0.03% C
0.01% Ta	0.0002% S	Ni Balance		

In order to study the influence of the V_c , f and the application of coolant in the temperature and the acquired signals, a Design Of Experiment (DOE) with two levels and 3 parameters was carried out. The two V_c tested were 15 and 30 m/min and the two f tested were 0.1 and 0.2 mm/rev. Changing the application of the coolant, with the selected cutting conditions both industrial and severe machining conditions were taken into account. In Table 2, the working conditions used in the drilling tests are shown.

Table 2 – Working conditions.

Working material	-	Inconel 718
	Hardness [±1] (HRC)	42 HRC
Cutting conditions	V_c (m/min)	15-30
	f (mm/rev)	0.1-0.2
	L (mm)	6.5
Tool	Material	Carbide
	Coating	TiAlN
	d_{drill} (mm)	8
	B_0 [±1] (º)	30
	$2\kappa_t$ (º)	140
	α [±1] (º)	8
	θ (in the middle of the radii) [±1] (º)	16
Coolant		Cutting oil / Dry
	Pressure	Low pressure
Machine-tool	Milling center	Lagun GVC 1000-HS
	CNC controller	Fagor 8070

For each of the working conditions analyzed in this study, 3 repetitions were done. It should be noted that as the wear increase after the drilling of one lubricated hole is negligible, it was assumed that the 3 externally lubricated holes drilled in each cutting condition were done under the same tool conditions. For the dry drilling condition tests, 3 holes were also drilled one after another. The first dry drilling of each cutting condition was done with a tool without wear, but as the dry conditions were so severe a gradual increase in drill wear was observed during the machining of the 3 holes. In this case, the level of error committed due to the tool wear increase was accepted (with a final mean VB~0.1 mm). Table 3 shows the experimental plan with the conditions employed in each test designed for this study.

Table 3 – Experimental plan.

Cutting Condition (CC)	V_c (m/min)	f (mm/rev)	Coolant/Irrigation	Cutting-Tool	Workpiece	Nº of repetitions
CC1	15	0.1	Yes	Drill 1	Test sample 1	3
CC2	15	0.1	No	Drill 1	Test sample 1	3
CC3	15	0.2	Yes	Drill 2	Test sample 2	3
CC4	15	0.2	No	Drill 2	Test sample 2	3
CC5	30	0.1	Yes	Drill 3	Test sample 3	3
CC6	30	0.1	No	Drill 3	Test sample 3	3
CC7	30	0.2	Yes	Drill 4	Test sample 4	3
CC8	30	0.2	No	Drill 4	Test sample 4	3

3. Theory and calculation

3.1. Calculation of the fraction of heat transferred to the workpiece (β)

A basic idea on heating in metal cutting is that temperature is a function of the fraction of heat to the chip and the ratio between the conductivity of the tool and workpiece [26]. Simplifying it can be said that:

$$T = f\left(\frac{h \cdot V_c}{\alpha_w}\right) \tag{1}$$

For the drilling process, it seems reasonable that the temperature of the side wall of the drilled hole depends on the heat partition between the chips and the workpiece, thus:

$$\Delta T_{\max}\left(\frac{\rho \cdot c}{K_s}\right) = f\left(\frac{h \cdot V_c}{\alpha_w}\right) \tag{2}$$

The workpieces were drilled at two cutting speeds and two feeds (Table 3). All the remaining parameters were kept unchanged as there are a number of approximations in the argument put forward here. For example if the drill geometry (e.g. point angle) changes it would result in torque variations, total cutting time variations and also the heat escape from beneath the drill to the sides would be different.

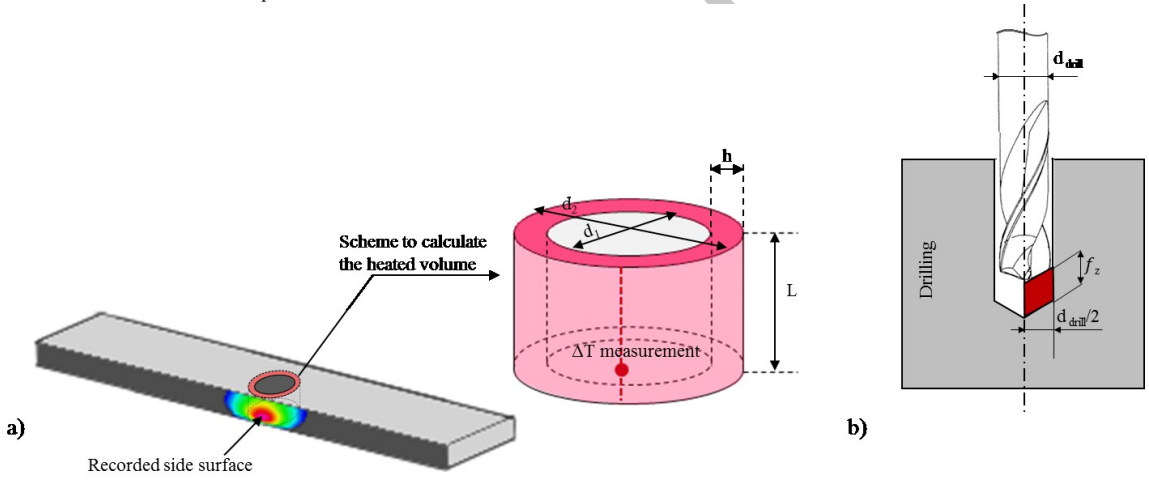

Fig. 3 – Schemes employed to calculate the (a) Heated volume (b) Removed material.

The thermal analysis was focused on the maximum heat transferred due to the fact that it will generate the maximum thermal damage in the workpiece. This parameter was calculated from the maximum workpiece temperatures measured experimentally with the infrared camera. To calculate the fraction of heat flowing into the workpiece some assumptions were made. The drilling heat flow may be considered to be transferred instantaneously to the surface of the drilled hole and after that spread by conduction. When the maximum temperature is reached the temperature gradients in the region between the hole and the recording surface will be at a minimum. The extent of the hot region filmed lies mainly within the 8 mm projected width of the drill. As shown in Fig. 3 (a), the amount of heat in the workpiece may be approximated to the amount in the cylindrical annulus, outer diameter (d_2=9 mm), inner diameter (d_1=8 mm) and height (L=6.5 mm). The outer diameter (d_2) is calculated as the sum of the drilled hole diameter (d_1) and twice the distance between the drilled hole and the infrared filming surface (h). Although the IR camera had been used to obtain a point surface temperature, this data could not have been obtained with a thermocouple due to the impossibility to know where the maximum temperatures would be achieved. In addition, the use of the IR camera allows to study if the temperature field extends beyond the outline of the drill. As explained later, this study would be necessary for the calculations carried out in this study.

$$Q_w = m \cdot c \cdot \Delta T_{\max} = L \cdot \rho \cdot (\pi/4) \cdot (d_2^2 - d_1^2) \cdot c \cdot \Delta T_{\max} \tag{3}$$

Once the $\Delta T_{\max}$ in the workpiece filming surface was obtained and for the Inconel 718 heat capacity $\rho \cdot c$, the heat in the workpiece was calculated (equation 3). Comparing with dry drilling, the heat evacuated by the cutting fluid will be reflected by the lower $\Delta T_{\max}$ achieved.

To calculate the specific cutting force, the cutting force must by divide by the cutting section. As shown in Fig. 3 (b), in the drilling process the cross-section area of work material removed by one cutting edge is equal to the feed per tooth multiplied by the number of teeth by the radius of the drill. The cutting force is obtained by dividing the experimentally obtained torque by the radial distance to the center of the cut cross-section area.

$$K_s = \frac{F_c}{S_c} = \frac{(M_z)/(\mathrm{d}_{drill}/4)}{(f_z \cdot z)\cdot(\mathrm{d}_{drill}/2)} = \frac{8 \cdot M_z}{(f_z \cdot z)\cdot \mathrm{d}_{drill}^{\,2}} \quad (4)$$

With the results of K_s, assuming that all the work is converted into heat and knowing that the work done in cutting is the specific cutting force multiplied by the volume removed by the drill, the heat generated with the drilling process (Q_{in}), is calculated as:

$$Q_{in} = W = (\pi/4)\cdot \mathrm{d}_{drill}^{\,2} \cdot L \cdot K_s \quad (5)$$

Once Q_{in} and Q_w are calculated, the fraction of generated heat flowing into the workpiece (β) is obtained (equation 6).

$$\beta = Q_w / Q_{in} \quad (6)$$

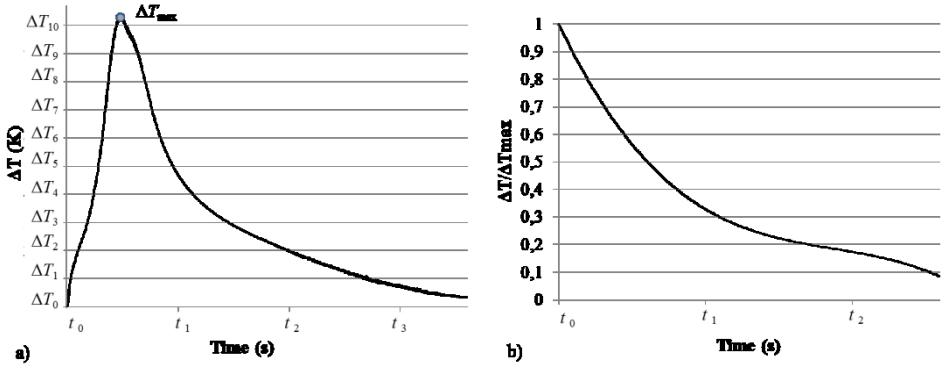

Fig. 4 – Theoretical curves (a) Temperature rise evolution during the drilling (b) Normalized cooling curve.

The β approximation could become poor as the time drilled increases. Heat released early in the drilling process will have time to conduct away before the hole is completed. In those cases, in order to obtain a correct β values it is important to take into account this heat. For that purpose ΔT_{max} may be adjusted to a larger value $(\Delta T_{max})_{adj}$ to allow for decay [21]. For that adjustment the normalized cooling curve must be calculated (Fig. 4 (b)). This curve is obtained considering the cooling part from the temperature rise curve where ΔT_{max} have been achieved (Fig. 4 (a)). $(\Delta T_{max})_{adj}$ is approximately calculated according to the area under the normalized cooling curve (Fig. 4 (b)), for t_0 to t_{cut}.

$$\frac{(\Delta T_{\max})_{adj}}{\Delta T_{\max}} = \frac{t_{cut}}{\int_0^{t_{cut}} (\Delta T/\Delta T_{\max})\, dt} \quad (7)$$

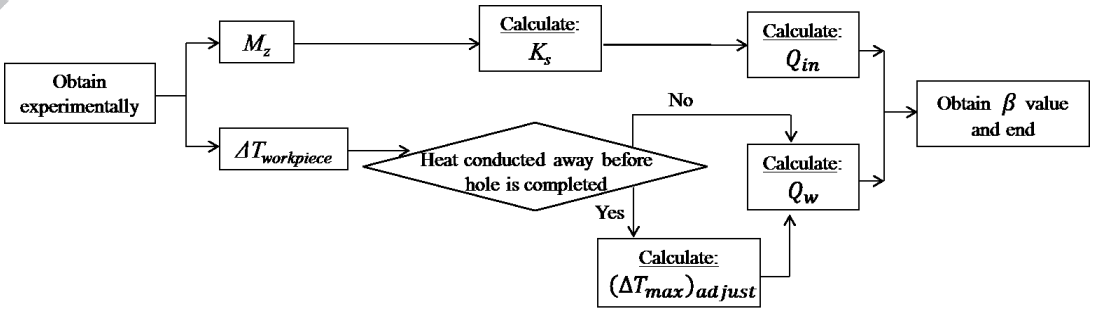

Fig. 5 – Flow diagram for determination of β.

To calculate the adjusted β, Q_w should be calculated again replacing ΔT_{max} with $(\Delta T_{max})_{adj}$ in equation 3. Finally, with the adjusted Q_w values the adjusted β values can be obtain as it is shown in equation 6.
Fig. 5 summarized in a flow diagram the model employed in this research to calculate the fraction of heat transferred to the workpiece.

3.2. Calculation of the Peclet number in drilling

The same dimensionless number that determines the proportion of heat carried away by the chip is known as the Peclet number (equation 8). In an orthogonal cutting operation (Fig. 6 (a)) *Pe* is determined by a cutting speed V_c and uncut chip thickness t_1 divided by the diffusivity of the workpiece material α_w [26].

$$Pe = \frac{V_c \cdot t_1}{\alpha_w} \tag{8}$$

In the drilling process this thermal number could be calculated as the product of the axial feed velocity and the drill diameter divided by the diffusivity (equation 9). The number gives the ratio of the time taken for the heat to diffuse a distance D in the workpiece (D^2/α_w) to the time taken for the drill to advance a distance D ($D/(z f_z \cdot \omega)$) [21] (Fig. 6 (b)). As the metal cutting theory states, the larger the ratio, smaller should be the proportion of heat that is transferred to the workpiece from beneath the advancing drill. Thus the portion of heat carried away by the chips is larger.

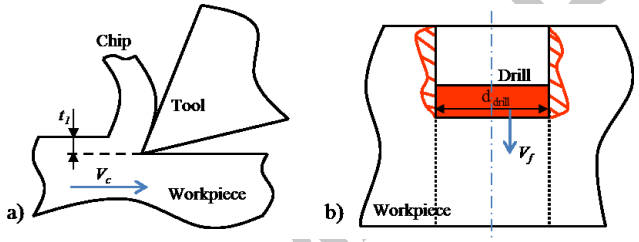

Fig. 6 – (a) Orthogonal cutting scheme (b) Drilling heat source moving scheme.

$$Pe = \frac{V_f \cdot d_{drill}}{\alpha_w} = \frac{(\omega \cdot z \cdot f_z) \cdot d_{drill}}{\alpha_w} \tag{9}$$

4. Results and discussion

4.1. Mechanical loads

In order to calculate the heat transferred to the workpiece, it is necessary to obtain M_z. In this case, the torque (M_z) was experimentally obtained as well as the feed force (F_z). A representative maximum value of M_z and F_z for each of the conditions tested was obtained as shown in Fig. 7.

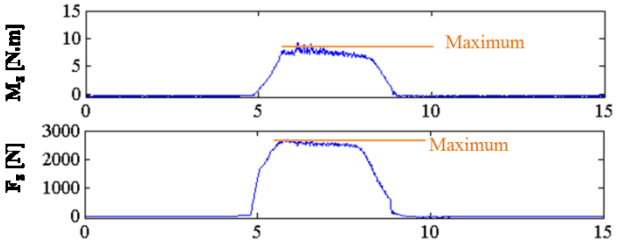

Fig. 7 – Externally lubricated V_c=15 m/min and f=0.2 mm/rev torque and feed force data.

From the maximum torque values the specific cutting force (K_s) was calculated. In Fig. 8 the obtained and calculated values are shown. As it can be observed (Fig. 8 a and b), regardless of the application of coolant, both torque and feed force describe the same trend. The maximum values were achieved with the lowest cutting speed (15 m/min) and the maximum feed (0.2 mm/rev). For 15 m/min the tendency of the values is to raise when the feed is increased. On the other hand, the lowest feed force and torque values were obtained with the highest cutting speed (30 m/min) and the lowest feed (0.1mm/rev). Although the values in this case are lower, the trend is the same as these of the lowest cutting speed, i.e., when the feed is increased, the values obtained rise. Focusing on the coolant application, the dry drilling showed higher values of torque and feed force. The only exception was the

V_c=15 m/min and f =0.2 mm/rev drilling condition. This fact is due to the higher values obtained in the second repetition of the lubricated drilling in this cutting condition (maybe because of a bad chip removal and a chip entrapment). This considerably increased the calculated mean value and the deviation showed in Fig. 8.

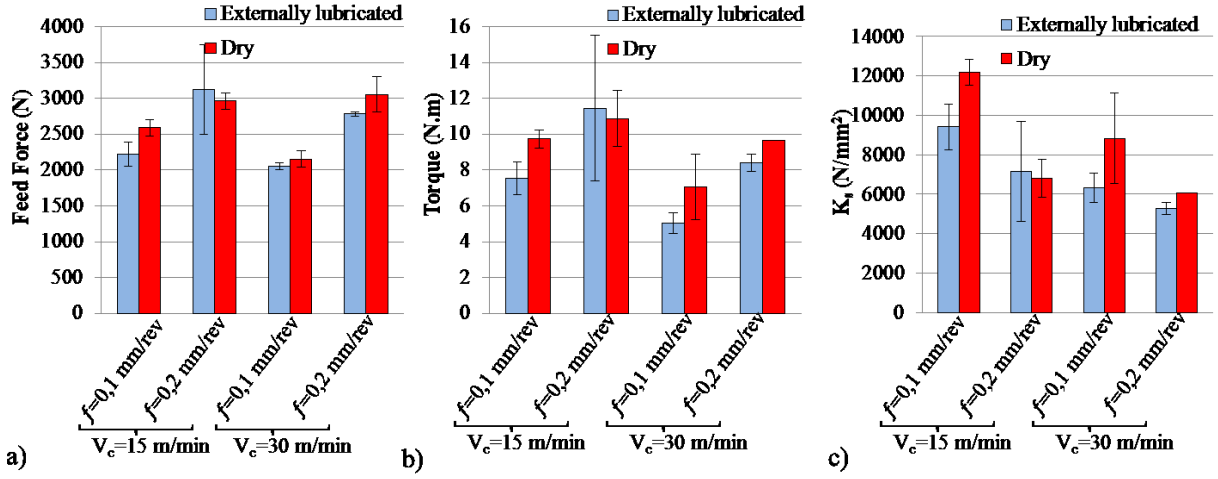

Fig. 8 –Mean of the maximum values obtained: (a) Torque (b) Feed force (b) Specific cutting force.

The effect of cutting speed and feed on the specific cutting force is shown in Fig. 8 c. The specific cutting force changes depending on the obtained cutting torque and the employed feed. As it is expected, the results show that the specific force decreased when the feed increase. In addition, the specific cutting force decreased as cutting speed increased at constant feed rate. This could be due to the reduction of the shear strength of the material caused by the increase of temperature in the cutting zone.

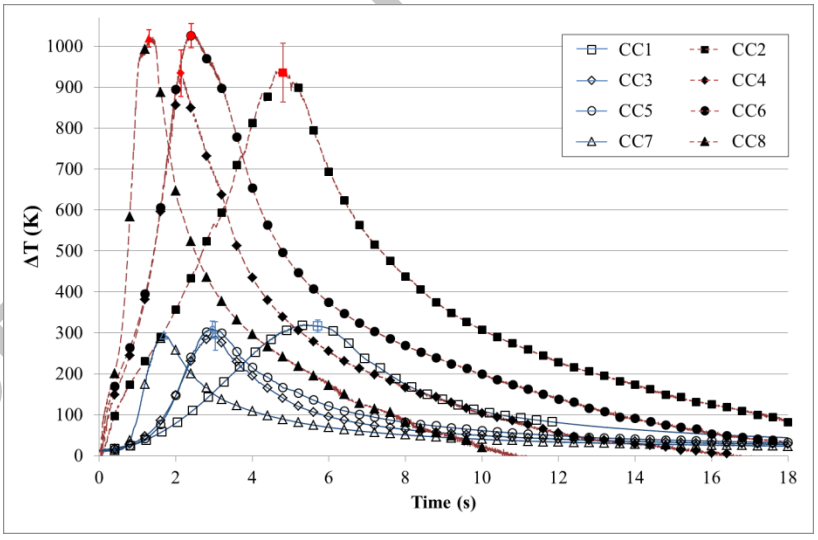

Fig. 9 – Mean of the maximum temperature rise evolution (open symbols belong to lubricated tests and solid symbols correspond to dry tests).

4.2. Thermal loads

The evolution of the temperature was obtained extracting the temperature information where the maximum temperature gradient was achieved (Fig. 3 (a)). A mean curve was calculated for each drilling condition tested (Fig. 9). As can be observed, the cutting temperature changed as the drill advances through the hole. In the case of the dry drilling holes, the temperature increased rapidly and signs of the high temperatures reached were seen (smoke and red-hot chips coming from the cutting zone and at the end of the process the near zone of the hole was red-hot).

Despite the external lubrication supply and the set-up that confined the workpiece and only allowed the lubrication to enter the cutting zone from the top of the hole, the temperatures measured in the lubricated tests decreased significantly compared to the dry drilling ones. This shows that the cutting heat spread rapidly from the cutting area and as a consequence the temperature significantly reduced.

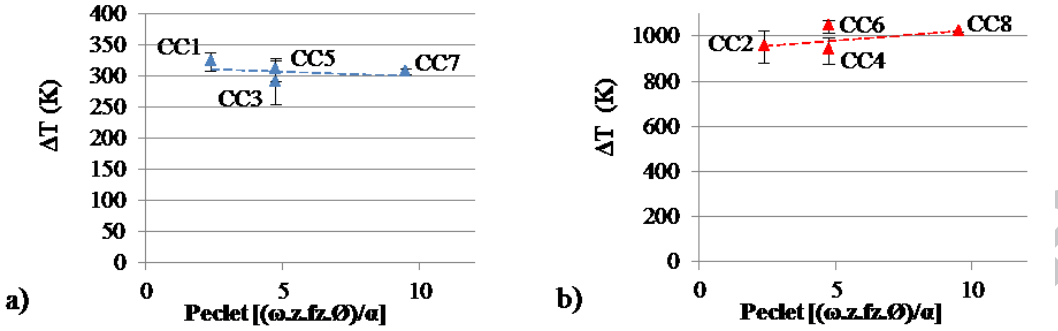

Fig. 10 –Maximum temperature rise at different Cutting Conditions (CC): (a) Lubricated tests (b) dry tests.

In Fig. 10 the maximum values of ΔT from Fig. 9, are plotted. Taking into account the uncertainty and deviations, in general terms it seems that as the dimensionless Peclet number (equation 9) increased, the tendency in lubricated and dry drilling scenario was different. In the lubricated tests as *Pe* increased (as the cutting speed and feed increased) the temperature increment decreased slightly. By contrast, in the dry drilling tests (regardless of the feed values), for *Pe* 4.7 and 9.4 (when the cutting speed was 30m/min) the temperature increase was the highest. However, for *Pe* values of 2.4 and 4.7 when the cutting speed was 15m/min the maximum ΔT were the lowest. These results show that the temperature observations are controversial when comparing the dry and lubricated scenarios. Hence, in order to obtain consistent conclusions the heat partition coefficient β was extracted.

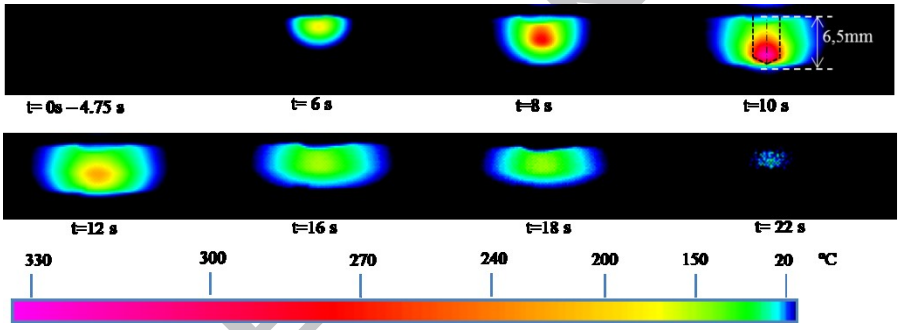

Fig. 11 – Temperature fields for the lubricated V_c=15 m/min and f=0.1 mm/rev test

4.3. Fraction of heat transferred to the workpiece

The temperature field at the recorded thermography time of maximum temperature, extends beyond the outline of the drill (t=10s in Fig. 11). In such cases a correction must be made in order to obtain the correct values of the heat partition. For that adjustment, the cooling curves obtained must be taken into consideration (Fig. 12). After the drilling process was finished, heat was conducted away from the heated parts at a cooling rate depending on the geometry of the region round the hole and the diffusivity of the workpiece. The maximum temperature reached should fall with time in a manner only weakly dependent on the cutting conditions (V_c and f) employed for the drilling [21]. However the curves obtained for dry and lubricated drilling test have very different gradients. Thus an adjustment for each different situation was made. In the Fig. 12 (a) and (b), the cooling portion of the data in Fig. 9 is shown. The x axis (time) has been offset to fix in each case the maximum temperature with the time t=0s.

To take into account the energy dissipated during the drilling due to the temperature field that extends beyond the outline of the drill at the time of maximum temperature (Fig. 11), $(\Delta T_{max})_{adj}$ was calculated. Thereby ΔT_{max} may be adjusted to a larger value $(\Delta T_{max})_{adj}$ to allow for decay [21]. As it is descried in equation (7), this value was approximately calculated according to the area under the curves of Fig. 12 (a) and (b), for t=0 to t_{cut}. With the $(\Delta T_{max})_{adj}$, Q was recalculated (equation 3) and finally the corrected β where obtained (equation 6).

In Fig. 13 the obtained fractions of heat transferred to the workpiece (β) against the Peclet number are plotted. Bearing in mind the assumed errors of the experimental tests and the approximations made to calculate β, the results for the lubricated tests show that the β values (after the adjustment) slightly decreased as the Peclet number increased. This is a physically feasible result and supports the view of a critical Peclet number below which increasing V_c and f_z lead to increasing temperatures in the workpiece and above which temperatures reduce (Fig. 10 a). By contrast, if it is not taken into account the energy dissipated during the drilling (before adjusted) the trend would be the opposite.

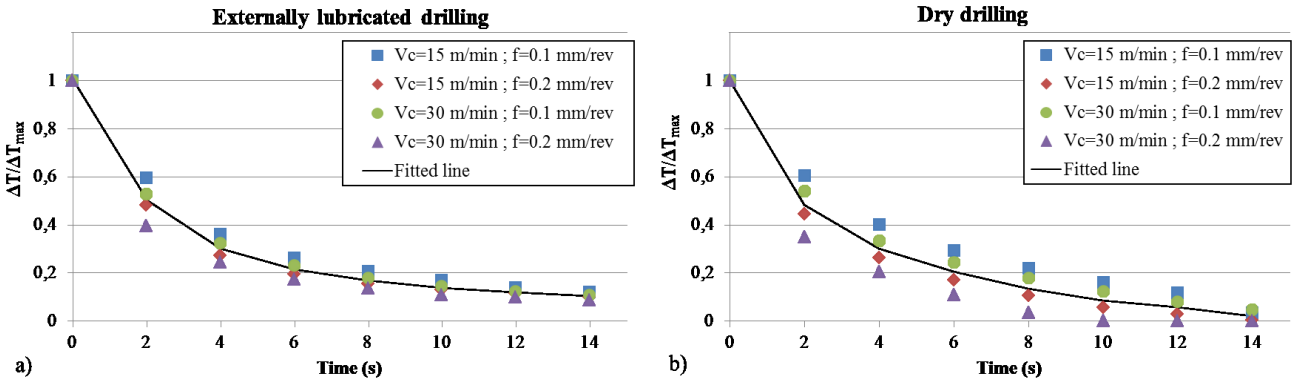

Fig. 12 – Normalized cooling curves (a) Lubricated tests (b) Dry tests.

On the other hand, β values on the dry drilling tests increased as the Peclet number does (both for the adjusted and not adjusted values). Based on theory, this was not the expected trend [26]. The heat flows to the workpiece proportionally to K_s. In the dry tests as the V_c and f increased, the K_s decreased and therefore β increased. The measured maximum temperatures on the workpiece also increased as the Peclet number did (Fig. 10 b). As it was stated, if chip extraction indexes decrease, the process temperatures increase due to the higher plastic deformation and friction caused by chip accumulation [32]. Analyzing the influence of the mechanical loads, the K_s is directly related with the obtained M_z value. The M_z results show the same trend observed by Kwong [33] where the M_z decreased as the cutting speed increased. So this unexpected increment in the β results could be derived from the severe machining cutting scenario tested. In tests carried out in dry conditions, problems such as inadequate chip removal, the friction derived from the interaction of the tool between the inner wall of the hole and the prevention of heat dissipation by the gasket could be the reason of the observed trend. All this was heightened by the set-up employed that confined the hole between the gaskets that would have resulted in problems related with the correct chip removal and heat dissipation. All this may have affected in an increase of the dry drilling β values as the energy introduced to the cutting process raised.

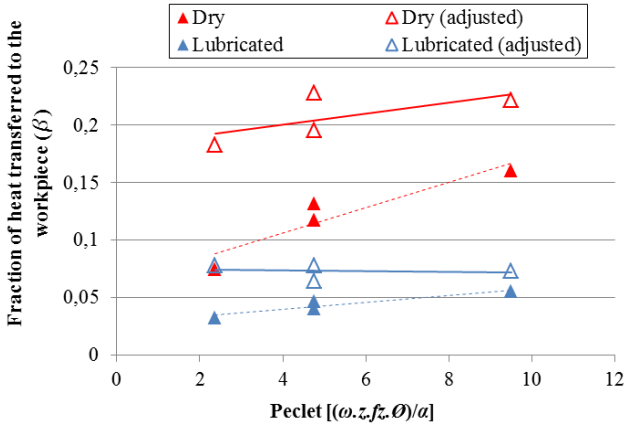

Fig. 13 – Fraction of heat transferred to the workpiece (β) plotted against Peclet number (adjusted (continuous line) and not adjusted (dashed line)).

The β values were also compared with the analytical values for the fraction of heat generated on the shear plane conducted to the workpiece (1-R_1) [15]. Where R_1:

$$R_1 = \frac{1}{\left(1+1.33\sqrt{\alpha_w \gamma_{sh}/V_c t_1}\right)} \qquad (10)$$

These analytical results ratified the decreasing trend observed with β in the lubricated tests and the values are close to the obtained ones (Fig. 13). As Pe increased the 1-R_1 fraction decreased (from a mean value of 0.08 for Pe=2.37 to 0.04 for Pe=9.49). These results are significantly lower than those obtained in the unlubricated drilling tests where signs of the high temperatures reached were detected. This would be caused because Loewen and Shaw's expression (equation 10) is limited to conditions where the influence on the temperature at the workpiece is limited to conditions in which the main heating source is the chip formation. In addition, this expression does not take into account the heat dissipated into the lubrication, so it is only valid for dry conditions. Therefore the equation does not take into account the additional heating due to the hole confinement and the problems to chip removal. It

should be highlighted that the β values obtained in this study considered both dry and lubricated drilling. The coolant greatly decreases the fraction of heat transferred to the workpiece in the ranges of $0.065 < \beta < 0.078$. Nevertheless, in the unlubricated conditions β was around 0.20. As result, it could be determined that for the lower (V_c=15 m/min; f=0.1 mm/rev, Pe =2.37) and highest (V_c=30 m/min; f=0.2 mm/rev, Pe =9.49) conditions tested, between 57% and 72% of the heat conducted to the workpiece could be reduced using the external oil lubrication.

It should be noted that the majority of the conditions employed by industry and by researchers for testing the Inconel 718 drilling process, are in Pe<10 conditions. When Pe<10 the deformation and friction energy affects the workpiece and alters the material properties [26]. A softening effect occurs that affects the plastic deformation during the cutting resulting in a reduction in the cutting forces. Taking this into account, it has been observed that both for feed force and torque, a clear trend could not be drawn to support this assertion. Moreover, for the tested conditions the calculated specific cutting forces are higher when Pe decreased.

As the surface integrity concern is so related to the machining of Inconel 718, not only the drilling process but also the finishing processes such as reaming should be specially considered. If Pe is calculated for a 6 teeth reamer working in V_c= 6 m/min and f= 0.2 mm/rev it gives an approximate value of 0.08. As it has been observed, this could result in a smaller portion of the heat generated in that process being transferred to the workpiece, but it is important to remember the importance of studying all the heat generation zones.

5. Conclusions

In this article the thermal loads measured by IR technique affecting the drilling of Inconel 718 have been studied. Four different cutting conditions in dry and lubricated scenario were analyzed. A model was employed to obtain the β values based on the torque and workpiece temperature measurements. The maximum β values were achieved in the unlubricated tests (around 0.20). By contrast, the coolant greatly decreases the heat rate transferred to the workpiece with β values ranging from 0.065 to 0.078 in dependence on the cutting speed and feed. These results show maximum β differences of 72% (V_c=30 m/min; f=0.2 mm/rev, Pe =9.49) and minimum of 57% (V_c=15 m/min; f=0.1 mm/rev, Pe =2.37). Despite the values obtained, these differences provide an order of magnitude of the heat transferred to the workpiece depending on the application or not application of coolant. Although sometimes is not that simple (as some other thermal parameters of the interface should be considered), the determined β values could be used as input parameters of analytical or numerical models.

Bearing in mind the assumed errors of the experimental tests and the approximations made to calculate β, the study presents the obtained trends of β relative to Peclet number that is dependent on the cutting speed and feed. In the lubricated tests, it was observed that β slightly decreased as the Peclet number increased. As observed in the bibliography, this is a physically feasible result. Unexpectedly, for the dry drilling tests β raised as Peclet increased. This fact ratified the complexity of the drilling process where it is important to considerer all the heat sources apart from the heat of the chip formation. As a conclusion it could be say that the cutting speeds and feed influence on the temperature at the workpiece is limited to conditions in which the main heating source is the chip formation.

Acknowledgements

The authors thank the Basque and Spanish Governments for the financial support given to the projects ESTRATEUS (IE14-396) and DESAFIO II (RTC-2014-1861-4).

The authors would like to thank Prof. Tom Childs, for his valuable inputs and comments to this paper.

References

[1] Ezugwu, E.; Bonney, J. & Yamane, Y. An overview of the machinability of aeroengine alloys Journal of Materials Processing Technology, 2003 , v 134 , n 2 , p 233 – 253

[2] Ulutan, D. & Ozel, T. Machining induced surface integrity in titanium and nickel alloys: A review International Journal of Machine Tools & Manufacture, 2011 , v 51 , n 3 , p 250 – 80

[3] Shaw, M. Metal cutting principles Oxford University Press Oxford, 1975 , v 19

[4] Liao, Y. & Shiue, R. Carbide tool wear mechanism in turning of Inconel 718 superalloy Wear, 1996 , v 193 , n 1 , p 16 – 24

[5] M'Saoubi, R.; Outeiro, J.; Chandrasekaran, H.; Dillon, O.W., J. & Jawahir, I. A review of surface integrity in machining and its impact on functional performance and life of machined products International Journal of Sustainable Manufacturing, 2008 , v 1 , n 1-2 , p 203 – 36

[6] Arrazola, P.-J.; Garay, A.; Fernandez, E. & Ostolaza, K. Correlation between tool flank wear, force signals and surface integrity when turning bars of Inconel 718 in finishing conditions International Journal of Machining and Machinability of Materials, Inderscience, 2014 , v 15 , n 1 , p 84-100

[7] Davim, J. Surface Integrity in Machining Springer, 2010

[8] Madariaga, A.; Esnaola, J.; Fernandez, E.; Arrazola, P.; Garay, A. & Morel, F. Analysis of residual stress and work-hardened profiles on Inconel 718 when face turning with large-nose radius tools International Journal of Advanced Manufacturing Technology, 2014 , v 71 , n 9-12 , p 1587 – 1598

[9] Pawade, R.; Joshi, S. S. & Brahmankar, P. Effect of machining parameters and cutting edge geometry on surface integrity of high-speed turned Inconel 718 International Journal of Machine Tools and Manufacture, 2008 , v 48 , n 1 , p 15 – 28

[10] Lopez de Lacalle, L.; Lamikiz, A.; Sanchez, J. & Arana, J. The effect of ball burnishing on heat-treated steel and Inconel 718 milled surfaces International Journal of Advanced Manufacturing Technology, 2007 , v 32 , n 9-10 , p 958 – 68

[11] Kwong, J.; Axinte, D. & Withers, P. The sensitivity of Ni-based superalloy to hole making operations: Influence of process parameters on subsurface damage and residual stress Journal of Materials Processing Technology, 2009 , v 209 , n 8 , p 3968 – 3977

[12] Dutilh, V.; Dessein, G.; Alexis, J. & Perrin, G. Links between machining parameters and surface integrity in drilling Ni-superalloy Advanced Materials Research, 2010 , v 112 , n 1 , p 171 – 178
[13] Le Coz, G.; Marinescu, M.; Devillez, A.; Dudzinski, D. & Velnom, L. Measuring temperature of rotating cutting tools: application to MQL drilling and dry milling of aerospace alloys Applied Thermal Engineering, 2012 , v 36 , p 434 – 41
[14] Stephenson, D. Assessment of steady-state metal cutting temperature models based on simultaneous infrared and thermocouple data Journal of Manufacturing Science and Engineering, American Society of Mechanical Engineers, 1991 , v 113 , n 2 , p 121-128
[15] Loewen, E. & Shaw, M. On the analysis of cutting tool temperatures Trans. ASME, 1954 , v 76 , n 2 , p 217-225
[16] Jaeger, J. C. Moving sources of heat and the temperature of sliding contacts J. and Proc. Roy. Soc. New South Wales, 1942 , v 76 , p 202
[17] Blok, H. Theoretical study of temperature rise at surfaces of actual contact under oiliness lubricating conditions Proceedings of the general discussion on lubrication and lubricants, 1937 , v 2 , p 222-235
[18] Agapiou, J. & DeVries, M. On the determination of thermal phenomena during drilling. Part I. Analytical models of twist drill temperature distributions International Journal of Machine Tools and Manufacture, 1990 , v 30 , n 2 , p 203 – 215
[19] Agapiou, J. & Stephenson, D. Analytical and experimental studies of drill temperatures Journal of engineering for industry, American Society of Mechanical Engineers, 1994 , v 116 , n 1 , p 54-60
[20] Bono, M. Thesis on experimental and analytical issues in drilling, The University of Michigan, 2001
[21] Soriano, J. M.; Garay, A.; Aristimuno, P.; Iriarte, L. M.; Eguren, J. A. & Arrazola, P. J. Efects of Rotational Speed, Feed Rate and Tool Type on Temperatures and Cutting Forces when drilling Bovine Cortical Bone Machining Science and Technology, Taylor & Francis, 2013 , v 17 , n 4 , p 611-636
[22] Yan, S.; Zhu, D.; Zhuang, K.; Zhang, X. & Ding, H. Modeling and analysis of coated tool temperature variation in dry milling of Inconel 718 turbine blade considering flank wear effect Journal of Materials Processing Technology, 2014 , v 214 , n 12 , p 2985 – 3001
[23] Stephenson, D. A. & Agapiou, J. S. Metal cutting theory and practice CRC press, 2006 , v 68
[24] Kronenberg, M. Machining science and application: theory and practice for operation and development of machining processes Pergamon Press, 1966
[25] Rech, J.; Arrazola, P.; Claudin, C.; Courbon, C.; Pusavec, F. & Kopac, J. Characterisation of friction and heat partition coefficients at the tool-work material interface in cutting CIRP Annals - Manufacturing Technology, 2013 , v 62 , n 1 , p 79 – 82
[26] Childs, T. Metal machining: theory and applications Hodder Arnold, 2000
[27] Fleischer, J.; Pabst, R. & Kelemen, S. Heat flow simulation for dry machining of power train castings CIRP Annals - Manufacturing Technology, 2007 , v 56 , n 1 , p 117 – 122
[28] Segurajauregui, U. & Arrazola, P. J. Heat-flow determination through inverse identification in drilling of aluminium workpieces with MQL Production Engineering, 2015
[29] Biermann, D. & Iovkov, I. Investigations on the thermal workpiece distortion in MQL deep hole drilling of an aluminium cast alloy CIRP Annals - Manufacturing Technology, 2015 , v 64 , n 1 , p 85 – 88
[30] Solter, J. & Gulpak, M. Heat partitioning in dry milling of steel CIRP Annals - Manufacturing Technology, 2012 , v 61 , n 1 , p 87 - 90
[31] Davies, M.; Ueda, T.; M'saoubi, R.; Mullany, B. & Cooke, A. On the measurement of temperature in material removal processes CIRP Annals-Manufacturing Technology, Elsevier, 2007 , v 56 , n 2 , p 581-604
[32] Brinksmeier, E.; Pecat, O. & Rentsch, R. Quantitative analysis of chip extraction in drilling of Ti6Al4V CIRP Annals - Manufacturing Technology, 2015 , v 64 , n 1 , p 93 - 96
[33] Kwong, J. Thesis on understanding the mechanisms affecting surface integrity during hole making operations on an advanced Ni-based superalloy, The University of Nottingham, 2009
[34] Beno, T. & Hulling, U. Measurement of cutting edge temperature in drilling Procedia CIRP, 2012 , v 3 , n 1 , p 531 – 536
[35] Okada, M.; Ueda, T.; Hosokawa, A. & Tanaka, R. Drilling of difficult-to-cut materials by using indexable insert drill with non-axisymmetrical geometry Nihon Kikai Gakkai Ronbunshu, C Hen/Transactions of the Japan Society of Mechanical Engineers, Part C, 2012 , v 78 , n 785 , p 252 – 261
[36] M'Saoubi, R.; Axinte, D.; Herbert, C.; Hardy, M. & Salmon, P. Surface integrity of nickel-based alloys subjected to severe plastic deformation by abusive drilling CIRP Annals-Manufacturing Technology, Elsevier, 2014 , v 63 , n 1 , p 61-64
[37] Soler, D.; Childs, T. H. & Arrazola, P. J. A Note on Interpreting Tool Temperature Measurements from Thermography Machining Science and Technology, Taylor & Francis, 2015 , v 19 , n 1 , p 174-181

Applied Thermal Engineering 00 (2015) 000–000

Available online at www.sciencedirect.com

SciVerse ScienceDirect

Journal homepage: www.journals.elsevier.com/applied-thermal-engineering/

HEAT TRANSFERRED TO THE WORKPIECE BASED ON TEMPERATURE MEASUREMENTS BY IR TECHNIQUE IN DRY AND LUBRICATED DRILLING OF INCONEL 718

M. Cuesta [a *], *P. Aristimuño* [a], *A. Garay* [a], *P. J. Arrazola* [a]

[a] *Faculty of Engineering, Mondragon University, Arrasate-Mondragón, Spain*

ARTICLE INFO

Article history:
Received 00 December 00
Received in revised form 00 January 00
Accepted 00 February 00

Keywords:
Heat partition
Infrared thermography
Inconel 718
Temperature
Drilling
Lubricated

ABSTRACT

In manufacturing aeronautical critical components, such as turbine discs commonly made of Inconel 718, surface integrity is crucial to ensure their fatigue life. Among the machining processes used, the drilling operation is one of the most critical as overheating can occur causing thermal damage to the hole. The amount of heat dissipated could determine the nature of deformation in the machining of Inconel 718. Nevertheless no detailed studies have determined experimentally the differences between the fractions of heat transferred to the workpiece (β) for dry and lubricated drilling. In this context, the thermal and mechanical loads (measured by IR technique and a piezoelectric dynamometer) affecting the drilling of Inconel 718 have been studied. Four different cutting conditions both in dry and lubricated conditions were tested. In order to obtain β, the study presents a model based on a new experimental method. The maximum β values were achieved in the unlubricated tests (around 0.20). By contrast, in the lubricated tests β range from 0.065 to 0.078. Therefore the fraction of heat conducted to the workpiece show maximum differences of 72% and minimum of 57% depending on the application or not application of coolant. Additionally, the obtained trends of β relative to Peclet number (that is dependent on the cutting speed, feed and drill diameter) are shown.

6. Introduction

Inconel 718 is one of the most used High Strength Thermal Resistant (HSTR) materials in the manufacturing of critical parts of aircraft engines such as turbine discs due to its high strength/weight ratio operating at extreme pressure and temperatures. However it is difficult to machine due to the inherent characteristics of the material such as the work hardening generated in the machining process, the low thermal conductivity or carbides presence [1, 3, 4]. Tool wear condition has a remarkable influence on Surface Integrity (SI), e.g., residual stresses, undesirable alteration of machined surfaces or induced strain loadings on the sub-surface, which in turn affect fatigue life of a component [5, 6]. For instance, it has been observed that different types of defects appeared on the machined component depending on whether the machining surface is affected mechanically, thermally or chemically [7]. Heat affected layers (phase transformation, cracking, white layer…) reduced greatly the fatigue performance of the machined parts. Furthermore the combination of high temperatures and high pressures induced high stresses that generate microstructural changes. It has been observed that while thermal dominant machining deformation induced tensile residual stresses in the machined surface, the mechanically dominant machining deformation induced compressive residual stresses [7, 8]. This effect might be in relationship with the amount of heat dissipation that determines the nature of deformation in the machining of Inconel 718 [9].

* *Corresponding author.* Tel.: +34-943-739-682 ; fax: +0-000-000-0000.
E-mail address: mcuesta@mondragon.edu (M. Cuesta)

xxxx-xxxx/$ – see front matter © 2015 Elsevier ltd. All rights reserved.
doi: xxxxxxxxxxxx

It should be highlighted that the majority of studies into the influences on surface integrity have focused on turning or milling [2, 6, 8, 9, 10]. The drilling process has largely been overlooked [11]. This is a surprising fact, as the holes are critical features with reference to fatigue performance [7]. This criticality is determined by two aspects; (i) the holes are critical geometrical features of the turbine discs and (ii) the drilling process itself. Due to its geometry, the holes are areas with high stress concentrations where the maximum stress values could be achieved. In that sense, it is important to prevent the thermal damage that could be caused by the overheating during the drilling due to an inadequate chip removal and the lack of lubrication. It is for these reasons that critical machined parts require a validation process to ensure the quality of the pieces in fatigue life. This validation generally involves freezing the cutting conditions by checking metallurgical analysis and fatigue tests to ensure that the cutting conditions are "safe". This process is complicated and involves high costs. Therefore, correlations between the cutting conditions and surface integrity would help to optimize manufacturing these components [12]. It is at this point that the monitoring and modelling of machining HSTR alloys plays a decisive role to solve problems related with the thermal loads [13].

Energetic balance distributions for machining processes have been studied since the 50's. Most of the models are based on the same physical laws and use the same hypothesis, usually with the main objective to determine the amount of heat transferred to the workpiece. Stephenson analyses different energetic balance models [14] and states that, Loewen and Shaw's heat distribution model [15] shows the best performance. This model treated the workpiece as a semi-infinite body subject to a heat flux imposed by a moving source of constant flux. It analyzes the 2D orthogonal cutting process based on Jaeger's frictional theory of the moving sources of sliding contacts [16] and Blok's principle of heat distribution [17].

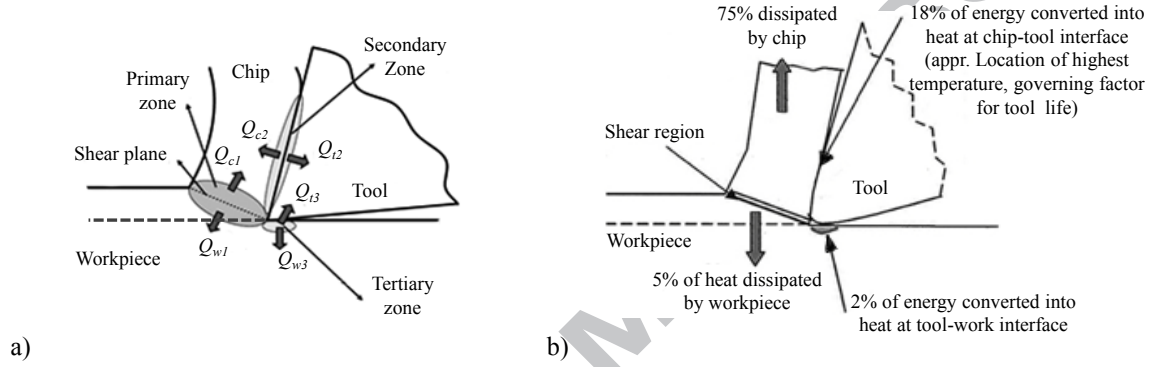

Fig. 1 – (a) Heat generation zones in cutting process (b) Typical energy distribution model in metal cutting at conventional speed [24].

Looking to the drilling process, thermal aspects have long been investigated from an analytical point of view [18, 19]. These studies are based on 2D orthogonal cutting theory and showed a general overview of the chip formation when drilling. Many of this researchers focused on evaluating and predicting the generation and flow of heat into the tool, the chips and the workpiece [20, 21, 22]. As it is shown in Fig.1 (a), the cutting heat is generated at three different deformation regions. Each zone has its own singularities, so the amount of heat that flows from each zone is different. In Fig. 1 (b) an example of heat dissipation in metal cutting is illustrated where approximately 25 % of energy from machining converts into heat. With this assumption, machining performance can be affected by the high thermal gradients. Temperature in primary deformation zone influences the mechanical properties of the workpiece. Whilst temperature at the secondary deformation zone strongly affects tool life [23], most of the heat generated in the tool-chip contact zone flows to the tool (around 18% of total heat [24]). This partial heat conducted to the tool leads to the tool temperature rise and the remaining heat is taken away by the fixed tool holder and the air [22]. Concerning to the workpiece, the transmitted cutting heat comes from the shear deformation zone. In Bonos advection heat partition model for drilling [20], all the heat generated on the shear plane is conducted directly into the workpiece. Thus, the heat generated by shearing is applied as a heat flux into the material below the cutting edge. This confirms that, as the drill moves into the workpiece, heat is continually added to the material so temperatures rarely reach a steady state and increase with the hole depth. Moreover, most of the models predict temperatures focus on the primary cutting edges, but other heat sources, such as friction between drill flutes and the workpiece or the influence of the chisel edge, should be taken into account.

The influence of temperature is more significant when machining HSTR alloys due to their heat resistance and poor thermal conductivity. Such thermal behavior must also be considered for understanding the distribution of residual stresses as high temperatures are well known to induce tensile stresses on the workpiece surface [7]. Rech et al. [25], tested on a special tribometer several materials including the Inconel 718. They employed different lubrication conditions and presented results and models for the portion of heat flux transmitted to the tool. Research works as this, give valuable information, but when the objective is to study the surface integrity and understand the influence of the different machining parameters, the focus should be put on the workpiece. In that line, Soriano et al. [21] studied the heat flow into the workpiece from the experimentally obtained workpiece temperatures (by IR technique) and cutting forces when dry drilling bovine cortical bone. The authors showed how the heat fractions decrease as the Peclet number increase. They conclude that this is a physically feasible result and supports the view of a critical Peclet number below which increasing cutting speed and feed lead to increasing temperatures in the workpiece and above which temperatures reduce. The Peclet number (frequently used in heat transfer theory) is widely used for thermal study of machining process. The heat transferred to the workpiece is controlled by Peclet number and the larger it is, the less heat escapes and the more is convected into the chip [26]. Related to this, Fleischer et al. showed an increase of the heat flux mainly caused by reducing the feed per tooth, ie. the undeformed chip thickness, when dry drilling of power train castings [27]. Segurajauregui and Arrazola [28] used the inverse simulation technique to calculate the heat input to the workpiece when drilling aluminium with MQL. They determined that an increase of the cutting speed and feed

rate leads to a decrease in heat input and temperature. Biermann and Iovkov [29] also concluded that the heat input to the workpiece could be significantly reduced increasing the feed values when deep hole drilling aluminium cast alloy applying MQL. Furthermore, the strong dependence of the heat flux and the heat partition to the workpiece on the undeformed chip thickness observed by Fleischer et al., was also detected when dry milling of steel [30].

Davies et al. in their review work stated that different methods such as thermocouples and infrared measurements have been used to study the temperatures in the drilling process [31]. Brinksmeier et al. [32] measured the process temperature when drilling Ti6Al4V with an infrared camera and showed a direct correlation between the process temperatures and the chip extraction at different conditions. With low chip extraction the chip accumulation caused a surface smoothening due to the interaction between the chip and the minor cutting edges. These conditions caused the increase in the cutting forces and temperatures due to intensive plastic deformation and friction. Focusing on the HSTR alloys, Kwong et al. [33] conducted a study of tool temperature drilling in severe conditions (VB=0, V_c=25m/min, f=0.10 rev/mm, dry) of the RR1000 HSTR alloy. They used the method of thermocouple inserted through the internal cooling of the drill. They measured temperatures of 750 °C. In that line, temperatures between 500-650ºC have been reported during drilling of Inconel 718 under severe conditions (VB=0.3, V_c=35m/min, f=0.12 and 0.05 rev/mm, dry) [34, 35]. Also temperature distribution of the numerical simulations carried out for Alloy 718, Waspalloy, Alloy 720Li and RR100 nickel-base superalloys showed maximum temperatures of 700ºC at the tool/workpiece interface [36]. As it can be seen, the majority of the studies analyzing temperature during the drilling of HSTR alloys have been focused on severe machining conditions (high material removal rates in dry cutting conditions). In addition, the temperatures analyzed usually correspond to the tool temperature. There have been no detailed investigations which obtained experimentally values of the heat transferred to the workpiece for externally lubricated drilling. And focusing on HSTR alloy drilling, no research has been found that studies the heat transferred to the workpiece. It is therefore interesting to deepen the study of the heat transferred to the workpiece while drilling dry and lubricated HSTR alloys.

The non-accepted thermally abused layers and the so called “white layers” can appear due the absence of coolant with or without and excessive tool wear [36]. Industrial surface quality standards specify that severe plastic deformations and/or thermally abused layers are not accepted on the Inconel 718 part surfaces drilled. In order to study the differences concerning the heat distribution in different scenarios, in this article, the temperature when drilling Inconel 718 with different cutting conditions in dry and externally lubricated have been studied. For that purpose a new experimental set-up was developed to enable the analysis of lubricated holes. To measure the workpiece temperature an infrared thermography (IR) camera was used. Thermography (thermal imaging) is a well-established experimental method for studying cutting tool [37] and workpiece [21] temperature distributions. The developed set-up enables to study the dry and lubricated drilling processes so the study of 4 different cutting conditions in dry and externally lubricated situations was done. Finally, the heat transferred to the workpiece for the tested different conditions was calculated.

Nomenclature

c	Specific heat (J/kg·K)
d_1	Generated hole diameter (mm)
d_2	Diameter of the heated cylinder (mm)
d_{drill}	Drill diameter (mm)
f	Feed per revolution (mm/rev)
f_z	Feed per tooth (mm/tooth)
F_z	Feed force (N)
F_{cut}	Cutting force (N)
h	Distance between the drilled hole and the infrared filming surface (mm)
K_s	Specific cutting force (N/mm^2)
L	Drilled depth (mm)
M_z	Torque (N.m)
Pe	Peclet number ( )
Q_{in}	Heat in introduced due to drilling process (J)
Q_c	Heat in the chip (J)
Q_t	Heat in the tool (J)
Q_w	Heat in the workpiece (J)
R_1	Fraction of heat generated on the shear plane conducted into the chip ( )
S_c	Cross section area of work material (mm^2)
t_{cut}	Cutting time (s)
t_1	Uncut chip thickness (mm)
V_f	Feed rate (mm/s)
V_c	Cutting speed (m/min)
VB	Average flank wear (mm)
W	Work done in cutting (J)
z	Teeth number ( )
α	Rake angle (º)
α_w	Workpiece diffusivity (m^2/s)
β	Fraction of generated heat flowing into the workpiece ( )

B_0	Helix angle (º)
γ_{sh}	Shear strain in the primary deformation zone
ΔT	Temperature increment (K)
$2\kappa_t$	Point angle (º)
θ	Clearance angle (º)
ρ	Density (kg/m^3)
ω	Rotational speed of the tool (rev/s)

7. Experimental procedure

7.1. Set-up, Measure Equipment and Methods

In this study, the temperature when drilling Inconel 718 in dry and externally lubricated condition was studied and a new experimental set-up was developed to enable the analysis of lubricated and unlubricated holes. The thermal phenomena of the workpiece were studied, as well as other typical machining parameters such as feed force (F_z) or torque (M_z). Fig. 2 (a) shows a diagram of the employed set-up for the drilling tests and Fig. 2 (b) shows a 3D detail of the analyzed zone. To measure the cutting forces (F_z and M_z), the drilled workpieces were clamped on a Kistler 9272 piezoelectric dynamometer. Test samples were plates machined to obtain perpendicular faces. Then, these samples were fixed on the top of the dynamometer and placed correctly in front of the FLIR Titanium 550 M IR camera 0.1 m away from the focus. The filming area (one of the side surfaces of the plates) can be observed in Fig. 2 (b). The length of this area was 40 mm and the height was delimitated by the depth (6.5 mm) of the test sample.

The objective was to study the thermal phenomena as close as possible to the cutting zone (the inner wall). In that sense, in order to avoid the lubrication to penetrate and disturb the recording wall, preliminary tests were carried out to define a minimum distance (h) between the drilled hole and the infrared filming surface (Fig. 2 (b)). This being so, the temperatures of the workpiece presented in this study were measured at a distance h=0.5 mm. The temperature rise (ΔT) of each test was extracted as the difference between the achieved maximum temperature and the temperature at the test starting moment. For each hole, all the data was extracted from one point where the maximum temperature gradients were achieved. In all the experimental tests presented the IR camera was set with a 12µm integration time and a frame rate of 500 Hz The procedure to obtain the temperature fields with the IR camera was the same described by Soriano et al. [21] and Segurajauregui and Arrazola [28].

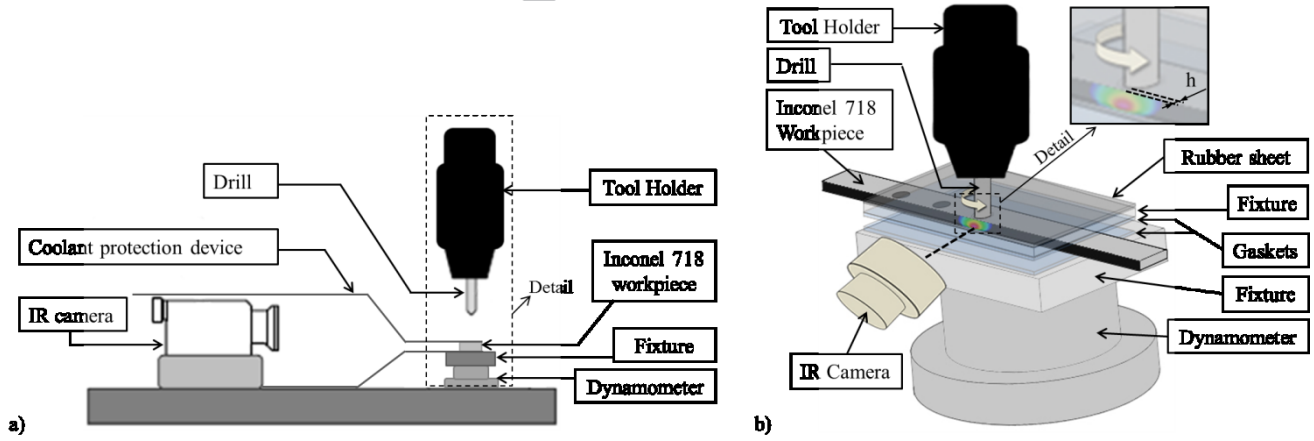

Fig. 2 –Experimental set-up (a) General scheme (b) 3D scheme of the detail in (a).

The signals from the dynamometer (F_z and M_z) were introduced in the analog input module of the machine. As result these signals were visualized and acquired at the same time with a 250 Hz frequency.

As shown in the Fig. 2 (a), a coolant protection device was designed for these tests. The device allowed the use of coolant in the externally lubricated tests, keeping dry the face where the IR camera was recording the heat flux. A detail with the 3D scheme of the solution developed to keep the recording wall dry is shown in Fig. 2 (b). For each test, while the Inconel 718 workpiece was drilled the upper and lower gaskets where also drilled. Thus the oil employed in the lubricated tests enters inside the hole, but did not wet the top of the workpiece and the recording wall.

The set-up was mounted in a vertical CNC milling center and was completed with a Kistler 5019 amplifier and the data analysis software.

7.2. Inconel 718 drilling tests

The workpiece material used for these tests was Inconel 718 rolled annealed and aged (AMS 5596). Each test sample was prepared in an EDM machine to obtain the final rectangular 20mm x 150 mm workpieces. Table 1 shows the chemical composition of the workpieces.

Table 1 – Chemical composition of the employed Inconel 718.

18.63% Cr	17.66% Fe	4.94% Nb	2.89% Mo	0.92% Ti
0.59% Al	0.24% Co	0.13% Si	0.12% Cu	0.03% C
0.01% Ta	0.0002% S	Ni Balance		

In order to study the influence of the V_c , f and the application of coolant in the temperature and the acquired signals, a Design Of Experiment (DOE) with two levels and 3 parameters was carried out. The two V_c tested were 15 and 30 m/min and the two f tested were 0.1 and 0.2 mm/rev. Changing the application of the coolant, with the selected cutting conditions both industrial and severe machining conditions were taken into account. In Table 2, the working conditions used in the drilling tests are shown.

Table 2 – Working conditions.

Working material	-	Inconel 718
	Hardness [±1] (HRC)	42 HRC
Cutting conditions	V_c (m/min)	15-30
	f (mm/rev)	0.1-0.2
	L (mm)	6.5
Tool	Material	Carbide
	Coating	TiAlN
	d_{drill} (mm)	8
	B_0 [±1] (º)	30
	$2\kappa_t$ (º)	140
	α [±1] (º)	8
	θ (in the middle of the radii) [±1] (º)	16
Coolant		Cutting oil / Dry
	Pressure	Low pressure
Machine-tool	Milling center	Lagun GVC 1000-HS
	CNC controller	Fagor 8070

For each of the working conditions analyzed in this study, 3 repetitions were done. It should be noted that as the wear increase after the drilling of one lubricated hole is negligible, it was assumed that the 3 externally lubricated holes drilled in each cutting condition were done under the same tool conditions. For the dry drilling condition tests, 3 holes were also drilled one after another. The first dry drilling of each cutting condition was done with a tool without wear, but as the dry conditions were so severe a gradual increase in drill wear was observed during the machining of the 3 holes. In this case, the level of error committed due to the tool wear increase was accepted (with a final mean VB~0.1 mm). Table 3 shows the experimental plan with the conditions employed in each test designed for this study.

Table 3 – Experimental plan.

Cutting Condition (CC)	V_c (m/min)	f (mm/rev)	Coolant/Irrigation	Cutting-Tool	Workpiece	Nº of repetitions
CC1	15	0.1	Yes	Drill 1	Test sample 1	3
CC2	15	0.1	No	Drill 1	Test sample 1	3
CC3	15	0.2	Yes	Drill 2	Test sample 2	3
CC4	15	0.2	No	Drill 2	Test sample 2	3
CC5	30	0.1	Yes	Drill 3	Test sample 3	3
CC6	30	0.1	No	Drill 3	Test sample 3	3
CC7	30	0.2	Yes	Drill 4	Test sample 4	3
CC8	30	0.2	No	Drill 4	Test sample 4	3

8. Theory and calculation

8.1. Calculation of the fraction of heat transferred to the workpiece (β)

A basic idea on heating in metal cutting is that temperature is a function of the fraction of heat to the chip and the ratio between the conductivity of the tool and workpiece [26]. Simplifying it can be said that:

$$T = f\left(\frac{h \cdot V_c}{\alpha_w}\right) \quad (1)$$

For the drilling process, it seems reasonable that the temperature of the side wall of the drilled hole depends on the heat partition between the chips and the workpiece, thus:

$$\Delta T_{\max}\left(\frac{\rho \cdot c}{K_s}\right) = f\left(\frac{h \cdot V_c}{\alpha_w}\right) \quad (2)$$

The workpieces were drilled at two cutting speeds and two feeds (Table 3). All the remaining parameters were kept unchanged as there are a number of approximations in the argument put forward here. For example if the drill geometry (e.g. point angle) changes it would result in torque variations, total cutting time variations and also the heat escape from beneath the drill to the sides would be different.

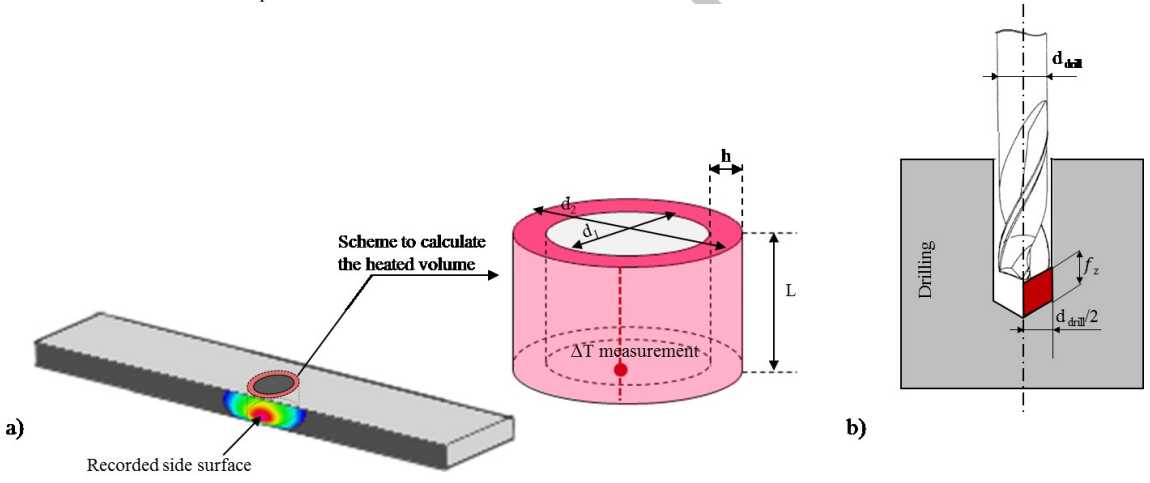

Fig. 3 – Schemes employed to calculate the (a) Heated volume (b) Removed material.

The thermal analysis was focused on the maximum heat transferred due to the fact that it will generate the maximum thermal damage in the workpiece. This parameter was calculated from the maximum workpiece temperatures measured experimentally with the infrared camera. To calculate the fraction of heat flowing into the workpiece some assumptions were made. The drilling heat flow may be considered to be transferred instantaneously to the surface of the drilled hole and after that spread by conduction. When the maximum temperature is reached the temperature gradients in the region between the hole and the recording surface will be at a minimum. The extent of the hot region filmed lies mainly within the 8 mm projected width of the drill. As shown in Fig. 3 (a), the amount of heat in the workpiece may be approximated to the amount in the cylindrical annulus, outer diameter (d_2=9 mm), inner diameter (d_1=8 mm) and height (L=6.5 mm). The outer diameter (d_2) is calculated as the sum of the drilled hole diameter (d_1) and twice the distance between the drilled hole and the infrared filming surface (h). Although the IR camera had been used to obtain a point surface temperature, this data could not have been obtained with a thermocouple due to the impossibility to know where the maximum temperatures would be achieved. In addition, the use of the IR camera allows to study if the temperature field extends beyond the outline of the drill. As explained later, this study would be necessary for the calculations carried out in this study.

$$Q_w = m \cdot c \cdot \Delta T_{\max} = L \cdot \rho \cdot (\pi/4) \cdot (d_2^2 - d_1^2) \cdot c \cdot \Delta T_{\max} \quad (3)$$

Once the $\Delta T_{\max}$ in the workpiece filming surface was obtained and for the Inconel 718 heat capacity $\rho \cdot c$, the heat in the workpiece was calculated (equation 3). Comparing with dry drilling, the heat evacuated by the cutting fluid will be reflected by the lower $\Delta T_{\max}$ achieved.

To calculate the specific cutting force, the cutting force must by divide by the cutting section. As shown in Fig. 3 (b), in the drilling process the cross-section area of work material removed by one cutting edge is equal to the feed per tooth multiplied by the number of teeth by the radius of the drill. The cutting force is obtained by dividing the experimentally obtained torque by the radial distance to the center of the cut cross-section area.

$$K_s = \frac{F_c}{S_c} = \frac{(M_z)/(\mathrm{d}_{drill}/4)}{(f_z \cdot z)\cdot(\mathrm{d}_{drill}/2)} = \frac{8 \cdot M_z}{(f_z \cdot z)\cdot \mathrm{d}_{drill}{}^2} \quad (4)$$

With the results of K_s, assuming that all the work is converted into heat and knowing that the work done in cutting is the specific cutting force multiplied by the volume removed by the drill, the heat generated with the drilling process (Q_{in}), is calculated as:

$$Q_{in} = W = (\pi/4)\cdot \mathrm{d}_{drill}{}^2 \cdot L \cdot K_s \quad (5)$$

Once Q_{in} and Q_w are calculated, the fraction of generated heat flowing into the workpiece (β) is obtained (equation 6).

$$\beta = Q_w / Q_{in} \quad (6)$$

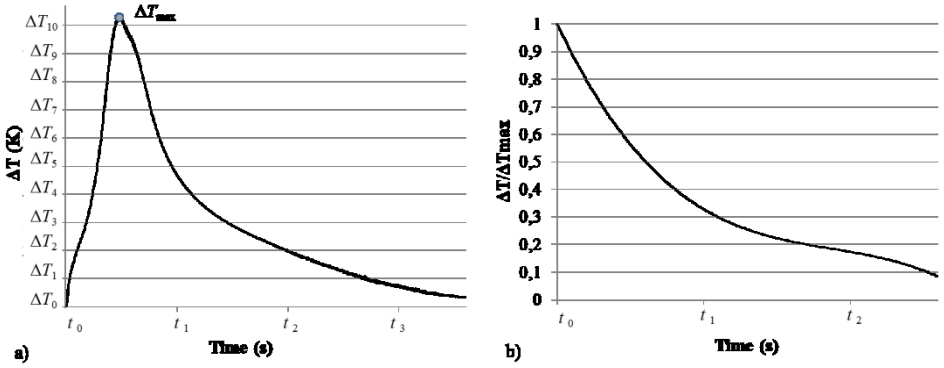

Fig. 4 – Theoretical curves (a) Temperature rise evolution during the drilling (b) Normalized cooling curve.

The β approximation could become poor as the time drilled increases. Heat released early in the drilling process will have time to conduct away before the hole is completed. In those cases, in order to obtain a correct β values it is important to take into account this heat. For that purpose ΔT_{max} may be adjusted to a larger value $(\Delta T_{max})_{adj}$ to allow for decay [21]. For that adjustment the normalized cooling curve must be calculated (Fig. 4 (b)). This curve is obtained considering the cooling part from the temperature rise curve where ΔT_{max} have been achieved (Fig. 4 (a)). $(\Delta T_{max})_{adj}$ is approximately calculated according to the area under the normalized cooling curve (Fig. 4 (b)), for t_0 to t_{cut}.

$$\frac{(\Delta T_{\max})_{adj}}{\Delta T_{\max}} = \frac{t_{cut}}{\int_0^{t_{cut}} (\Delta T/\Delta T_{\max})\, dt} \quad (7)$$

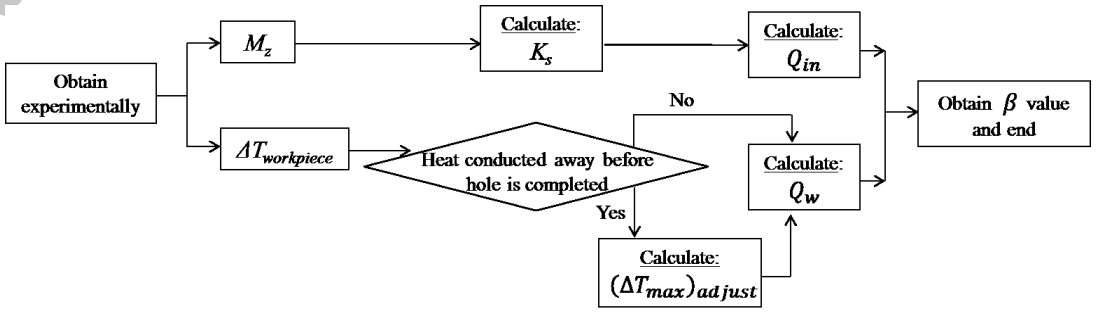

Fig. 5 – Flow diagram for determination of β.

To calculate the adjusted β, Q_w should be calculated again replacing ΔT_{max} with $(\Delta T_{max})_{adj}$ in equation 3. Finally, with the adjusted Q_w values the adjusted β values can be obtain as it is shown in equation 6.
Fig. 5 summarized in a flow diagram the model employed in this research to calculate the fraction of heat transferred to the workpiece.

8.2. Calculation of the Peclet number in drilling

The same dimensionless number that determines the proportion of heat carried away by the chip is known as the Peclet number (equation 8). In an orthogonal cutting operation (Fig. 6 (a)) *Pe* is determined by a cutting speed V_c and uncut chip thickness t_1 divided by the diffusivity of the workpiece material α_w [26].

$$Pe = \frac{V_c \cdot t_1}{\alpha_w} \tag{8}$$

In the drilling process this thermal number could be calculated as the product of the axial feed velocity and the drill diameter divided by the diffusivity (equation 9). The number gives the ratio of the time taken for the heat to diffuse a distance D in the workpiece (D^2/α_w) to the time taken for the drill to advance a distance D ($D/(z \cdot f_z \cdot \omega)$) [21] (Fig. 6 (b)). As the metal cutting theory states, the larger the ratio, smaller should be the proportion of heat that is transferred to the workpiece from beneath the advancing drill. Thus the portion of heat carried away by the chips is larger.

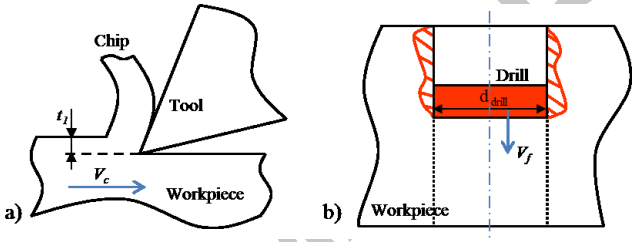

Fig. 6 – (a) Orthogonal cutting scheme (b) Drilling heat source moving scheme.

$$Pe = \frac{V_f \cdot d_{drill}}{\alpha_w} = \frac{(\omega \cdot z \cdot f_z) \cdot d_{drill}}{\alpha_w} \tag{9}$$

9. Results and discussion

9.1. Mechanical loads

In order to calculate the heat transferred to the workpiece, it is necessary to obtain M_z. In this case, the torque (M_z) was experimentally obtained as well as the feed force (F_z). A representative maximum value of M_z and F_z for each of the conditions tested was obtained as shown in Fig. 7.

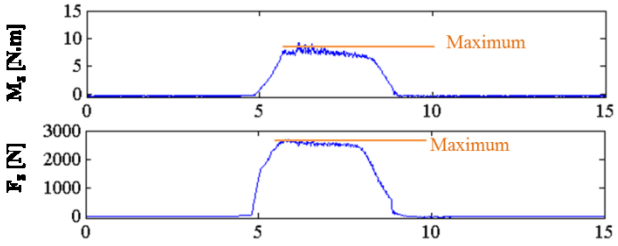

Fig. 7 – Externally lubricated V_c=15 m/min and f=0.2 mm/rev torque and feed force data.

From the maximum torque values the specific cutting force (K_s) was calculated. In Fig. 8 the obtained and calculated values are shown. As it can be observed (Fig. 8 a and b), regardless of the application of coolant, both torque and feed force describe the same trend. The maximum values were achieved with the lowest cutting speed (15 m/min) and the maximum feed (0.2 mm/rev). For 15 m/min the tendency of the values is to raise when the feed is increased. On the other hand, the lowest feed force and torque values were obtained with the highest cutting speed (30 m/min) and the lowest feed (0.1mm/rev). Although the values in this case are lower, the trend is the same as these of the lowest cutting speed, i.e., when the feed is increased, the values obtained rise. Focusing on the coolant application, the dry drilling showed higher values of torque and feed force. The only exception was the

V_c=15 m/min and f =0.2 mm/rev drilling condition. This fact is due to the higher values obtained in the second repetition of the lubricated drilling in this cutting condition (maybe because of a bad chip removal and a chip entrapment). This considerably increased the calculated mean value and the deviation showed in Fig. 8.

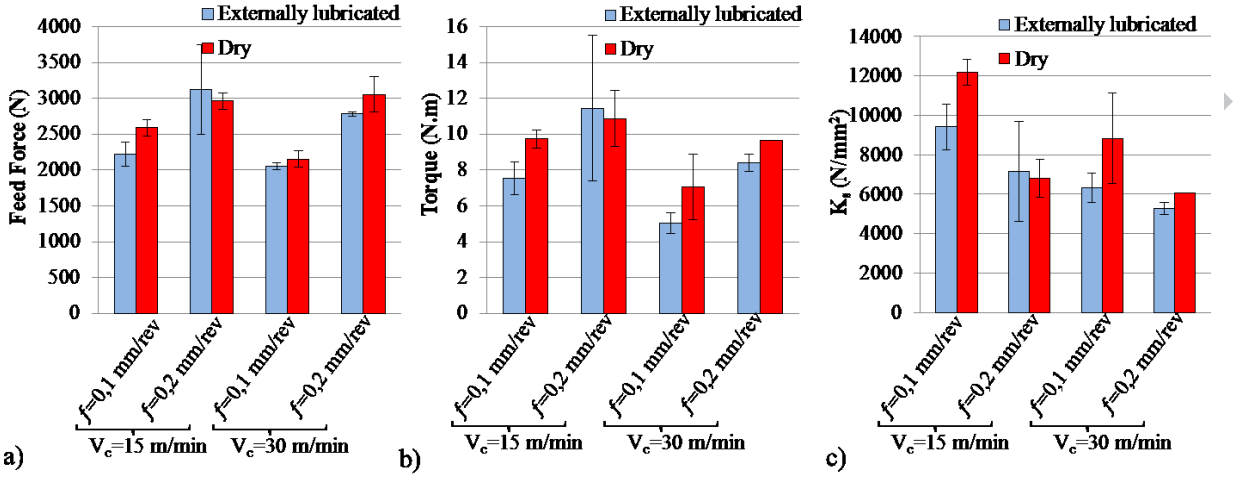

Fig. 8 –Mean of the maximum values obtained: (a) Torque (b) Feed force (b) Specific cutting force.

The effect of cutting speed and feed on the specific cutting force is shown in Fig. 8 c. The specific cutting force changes depending on the obtained cutting torque and the employed feed. As it is expected, the results show that the specific force decreased when the feed increase. In addition, the specific cutting force decreased as cutting speed increased at constant feed rate. This could be due to the reduction of the shear strength of the material caused by the increase of temperature in the cutting zone.

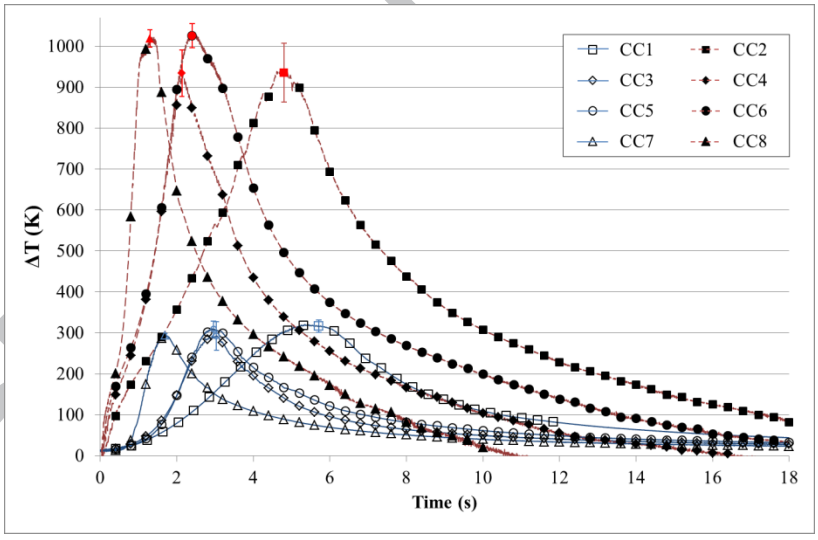

Fig. 9 – Mean of the maximum temperature rise evolution (open symbols belong to lubricated tests and solid symbols correspond to dry tests).

9.2. Thermal loads

The evolution of the temperature was obtained extracting the temperature information where the maximum temperature gradient was achieved (Fig. 3 (a)). A mean curve was calculated for each drilling condition tested (Fig. 9). As can be observed, the cutting temperature changed as the drill advances through the hole. In the case of the dry drilling holes, the temperature increased rapidly and signs of the high temperatures reached were seen (smoke and red-hot chips coming from the cutting zone and at the end of the process the near zone of the hole was red-hot).

Despite the external lubrication supply and the set-up that confined the workpiece and only allowed the lubrication to enter the cutting zone from the top of the hole, the temperatures measured in the lubricated tests decreased significantly compared to the dry drilling ones. This shows that the cutting heat spread rapidly from the cutting area and as a consequence the temperature significantly reduced.

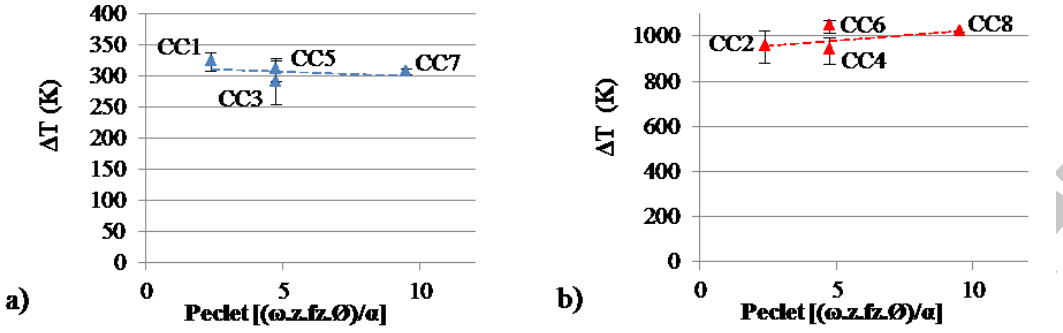

Fig. 10 –Maximum temperature rise at different Cutting Conditions (CC): (a) Lubricated tests (b) dry tests.

In Fig. 10 the maximum values of ΔT from Fig. 9, are plotted. Taking into account the uncertainty and deviations, in general terms it seems that as the dimensionless Peclet number (equation 9) increased, the tendency in lubricated and dry drilling scenario was different. In the lubricated tests as *Pe* increased (as the cutting speed and feed increased) the temperature increment decreased slightly. By contrast, in the dry drilling tests (regardless of the feed values), for *Pe* 4.7 and 9.4 (when the cutting speed was 30m/min) the temperature increase was the highest. However, for *Pe* values of 2.4 and 4.7 when the cutting speed was 15m/min the maximum ΔT were the lowest. These results show that the temperature observations are controversial when comparing the dry and lubricated scenarios. Hence, in order to obtain consistent conclusions the heat partition coefficient β was extracted.

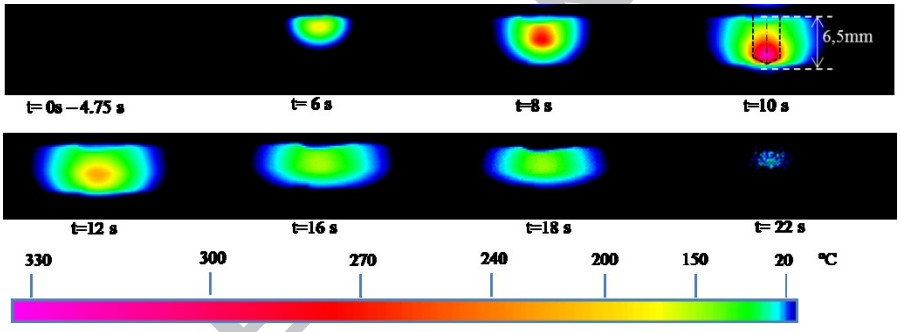

Fig. 11 – Temperature fields for the lubricated V_c=15 m/min and f=0.1 mm/rev test

9.3. Fraction of heat transferred to the workpiece

The temperature field at the recorded thermography time of maximum temperature, extends beyond the outline of the drill (t=10s in Fig. 11). In such cases a correction must be made in order to obtain the correct values of the heat partition. For that adjustment, the cooling curves obtained must be taken into consideration (Fig. 12). After the drilling process was finished, heat was conducted away from the heated parts at a cooling rate depending on the geometry of the region round the hole and the diffusivity of the workpiece. The maximum temperature reached should fall with time in a manner only weakly dependent on the cutting conditions (V_c and f) employed for the drilling [21]. However the curves obtained for dry and lubricated drilling test have very different gradients. Thus an adjustment for each different situation was made. In the Fig. 12 (a) and (b), the cooling portion of the data in Fig. 9 is shown. The x axis (time) has been offset to fix in each case the maximum temperature with the time t=0s.

To take into account the energy dissipated during the drilling due to the temperature field that extends beyond the outline of the drill at the time of maximum temperature (Fig. 11), $(\Delta T_{max})_{adj}$ was calculated. Thereby ΔT_{max} may be adjusted to a larger value $(\Delta T_{max})_{adj}$ to allow for decay [21]. As it is descried in equation (7), this value was approximately calculated according to the area under the curves of Fig. 12 (a) and (b), for t=0 to t_{cut}. With the $(\Delta T_{max})_{adj}$, Q was recalculated (equation 3) and finally the corrected β where obtained (equation 6).

In Fig. 13 the obtained fractions of heat transferred to the workpiece (β) against the Peclet number are plotted. Bearing in mind the assumed errors of the experimental tests and the approximations made to calculate β, the results for the lubricated tests show that the β values (after the adjustment) slightly decreased as the Peclet number increased. This is a physically feasible result and supports the view of a critical Peclet number below which increasing V_c and f_z lead to increasing temperatures in the workpiece and above which temperatures reduce (Fig. 10 a). By contrast, if it is not taken into account the energy dissipated during the drilling (before adjusted) the trend would be the opposite.

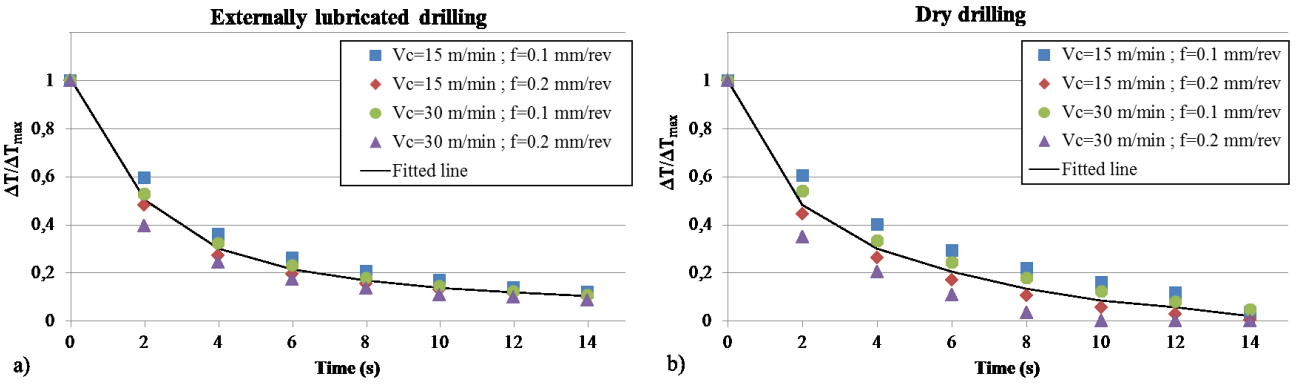

Fig. 12 – Normalized cooling curves (a) Lubricated tests (b) Dry tests.

On the other hand, β values on the dry drilling tests increased as the Peclet number does (both for the adjusted and not adjusted values). Based on theory, this was not the expected trend [26]. The heat flows to the workpiece proportionally to K_s. In the dry tests as the V_c and f increased, the K_s decreased and therefore β increased. The measured maximum temperatures on the workpiece also increased as the Peclet number did (Fig. 10 b). As it was stated, if chip extraction indexes decrease, the process temperatures increase due to the higher plastic deformation and friction caused by chip accumulation [32]. Analyzing the influence of the mechanical loads, the K_s is directly related with the obtained M_z value. The M_z results show the same trend observed by Kwong [33] where the M_z decreased as the cutting speed increased. So this unexpected increment in the β results could be derived from the severe machining cutting scenario tested. In tests carried out in dry conditions, problems such as inadequate chip removal, the friction derived from the interaction of the tool between the inner wall of the hole and the prevention of heat dissipation by the gasket could be the reason of the observed trend. All this was heightened by the set-up employed that confined the hole between the gaskets that would have resulted in problems related with the correct chip removal and heat dissipation. All this may have affected in an increase of the dry drilling β values as the energy introduced to the cutting process raised.

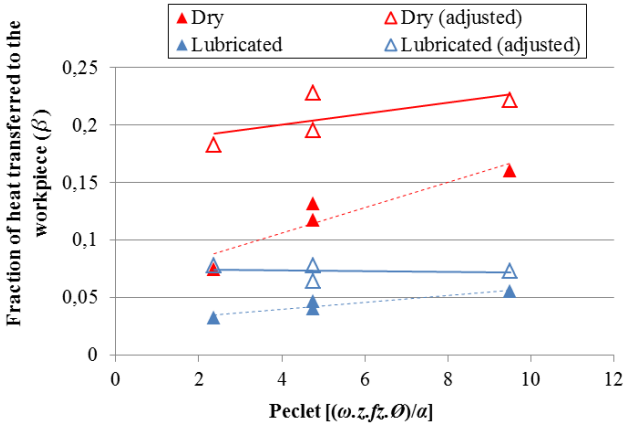

Fig. 13 – Fraction of heat transferred to the workpiece (β) plotted against Peclet number (adjusted (continuous line) and not adjusted (dashed line)).

The β values were also compared with the analytical values for the fraction of heat generated on the shear plane conducted to the workpiece (1-R_1) [15]. Where R_1:

$$R_1 = \frac{1}{\left(1+1.33\sqrt{\alpha_w \gamma_{sh}/V_c t_1}\right)} \qquad (10)$$

These analytical results ratified the decreasing trend observed with β in the lubricated tests and the values are close to the obtained ones (Fig. 13). As Pe increased the 1-R_1 fraction decreased (from a mean value of 0.08 for Pe=2.37 to 0.04 for Pe=9.49). These results are significantly lower than those obtained in the unlubricated drilling tests where signs of the high temperatures reached were detected. This would be caused because Loewen and Shaw's expression (equation 10) is limited to conditions where the influence on the temperature at the workpiece is limited to conditions in which the main heating source is the chip formation. In addition, this expression does not take into account the heat dissipated into the lubrication, so it is only valid for dry conditions. Therefore the equation does not take into account the additional heating due to the hole confinement and the problems to chip removal. It

should be highlighted that the β values obtained in this study considered both dry and lubricated drilling. The coolant greatly decreases the fraction of heat transferred to the workpiece in the ranges of $0.065 < \beta < 0.078$. Nevertheless, in the unlubricated conditions β was around 0.20. As result, it could be determined that for the lower (V_c=15 m/min; f=0.1 mm/rev, Pe =2.37) and highest (V_c=30 m/min; f=0.2 mm/rev, Pe =9.49) conditions tested, between 57% and 72% of the heat conducted to the workpiece could be reduced using the external oil lubrication.

It should be noted that the majority of the conditions employed by industry and by researchers for testing the Inconel 718 drilling process, are in Pe<10 conditions. When Pe<10 the deformation and friction energy affects the workpiece and alters the material properties [26]. A softening effect occurs that affects the plastic deformation during the cutting resulting in a reduction in the cutting forces. Taking this into account, it has been observed that both for feed force and torque, a clear trend could not be drawn to support this assertion. Moreover, for the tested conditions the calculated specific cutting forces are higher when Pe decreased.

As the surface integrity concern is so related to the machining of Inconel 718, not only the drilling process but also the finishing processes such as reaming should be specially considered. If Pe is calculated for a 6 teeth reamer working in V_c= 6 m/min and f= 0.2 mm/rev it gives an approximate value of 0.08. As it has been observed, this could result in a smaller portion of the heat generated in that process being transferred to the workpiece, but it is important to remember the importance of studying all the heat generation zones.

10. Conclusions

In this article the thermal loads measured by IR technique affecting the drilling of Inconel 718 have been studied. Four different cutting conditions in dry and lubricated scenario were analyzed. A model was employed to obtain the β values based on the torque and workpiece temperature measurements. The maximum β values were achieved in the unlubricated tests (around 0.20). By contrast, the coolant greatly decreases the heat rate transferred to the workpiece with β values ranging from 0.065 to 0.078 in dependence on the cutting speed and feed. These results show maximum β differences of 72% (V_c=30 m/min; f=0.2 mm/rev, Pe =9.49) and minimum of 57% (V_c=15 m/min; f=0.1 mm/rev, Pe =2.37). Despite the values obtained, these differences provide an order of magnitude of the heat transferred to the workpiece depending on the application or not application of coolant. Although sometimes is not that simple (as some other thermal parameters of the interface should be considered), the determined β values could be used as input parameters of analytical or numerical models.

Bearing in mind the assumed errors of the experimental tests and the approximations made to calculate β, the study presents the obtained trends of β relative to Peclet number that is dependent on the cutting speed and feed. In the lubricated tests, it was observed that β slightly decreased as the Peclet number increased. As observed in the bibliography, this is a physically feasible result. Unexpectedly, for the dry drilling tests β raised as Peclet increased. This fact ratified the complexity of the drilling process where it is important to considerer all the heat sources apart from the heat of the chip formation. As a conclusion it could be say that the cutting speeds and feed influence on the temperature at the workpiece is limited to conditions in which the main heating source is the chip formation.

Acknowledgements

The authors thank the Basque and Spanish Governments for the financial support given to the projects ESTRATEUS (IE14-396) and DESAFIO II (RTC-2014-1861-4).

The authors would like to thank Prof. Tom Childs, for his valuable inputs and comments to this paper.

REFERENCES

[1] Ezugwu, E.; Bonney, J. & Yamane, Y. An overview of the machinability of aeroengine alloys Journal of Materials Processing Technology, 2003 , v 134 , n 2 , p 233 – 253

[2] Ulutan, D. & Ozel, T. Machining induced surface integrity in titanium and nickel alloys: A review International Journal of Machine Tools & Manufacture, 2011 , v 51 , n 3 , p 250 – 80

[3] Shaw, M. Metal cutting principles Oxford University Press Oxford, 1975 , v 19

[4] Liao, Y. & Shiue, R. Carbide tool wear mechanism in turning of Inconel 718 superalloy Wear, 1996 , v 193 , n 1 , p 16 – 24

[5] M'Saoubi, R.; Outeiro, J.; Chandrasekaran, H.; Dillon, O.W., J. & Jawahir, I. A review of surface integrity in machining and its impact on functional performance and life of machined products International Journal of Sustainable Manufacturing, 2008 , v 1 , n 1-2 , p 203 – 36

[6] Arrazola, P.-J.; Garay, A.; Fernandez, E. & Ostolaza, K. Correlation between tool flank wear, force signals and surface integrity when turning bars of Inconel 718 in finishing conditions International Journal of Machining and Machinability of Materials, Inderscience, 2014 , v 15 , n 1 , p 84-100

[7] Davim, J. Surface Integrity in Machining Springer, 2010

[8] Madariaga, A.; Esnaola, J.; Fernandez, E.; Arrazola, P.; Garay, A. & Morel, F. Analysis of residual stress and work-hardened profiles on Inconel 718 when face turning with large-nose radius tools International Journal of Advanced Manufacturing Technology, 2014 , v 71 , n 9-12 , p 1587 – 1598

[9] Pawade, R.; Joshi, S. S. & Brahmankar, P. Effect of machining parameters and cutting edge geometry on surface integrity of high-speed turned Inconel 718 International Journal of Machine Tools and Manufacture, 2008 , v 48 , n 1 , p 15 – 28

[10] Lopez de Lacalle, L.; Lamikiz, A.; Sanchez, J. & Arana, J. The effect of ball burnishing on heat-treated steel and Inconel 718 milled surfaces International Journal of Advanced Manufacturing Technology, 2007 , v 32 , n 9-10 , p 958 – 68

[11] Kwong, J.; Axinte, D. & Withers, P. The sensitivity of Ni-based superalloy to hole making operations: Influence of process parameters on subsurface damage and residual stress Journal of Materials Processing Technology, 2009 , v 209 , n 8 , p 3968 – 3977

[12] Dutilh, V.; Dessein, G.; Alexis, J. & Perrin, G. Links between machining parameters and surface integrity in drilling Ni-superalloy Advanced Materials Research, 2010 , v 112 , n 1 , p 171 – 178
[13] Le Coz, G.; Marinescu, M.; Devillez, A.; Dudzinski, D. & Velnom, L. Measuring temperature of rotating cutting tools: application to MQL drilling and dry milling of aerospace alloys Applied Thermal Engineering, 2012 , v 36 , p 434 – 41
[14] Stephenson, D. Assessment of steady-state metal cutting temperature models based on simultaneous infrared and thermocouple data Journal of Manufacturing Science and Engineering, American Society of Mechanical Engineers, 1991 , v 113 , n 2 , p 121-128
[15] Loewen, E. & Shaw, M. On the analysis of cutting tool temperatures Trans. ASME, 1954 , v 76 , n 2 , p 217-225
[16] Jaeger, J. C. Moving sources of heat and the temperature of sliding contacts J. and Proc. Roy. Soc. New South Wales, 1942 , v 76 , p 202
[17] Blok, H. Theoretical study of temperature rise at surfaces of actual contact under oiliness lubricating conditions Proceedings of the general discussion on lubrication and lubricants, 1937 , v 2 , p 222-235
[18] Agapiou, J. & DeVries, M. On the determination of thermal phenomena during drilling. Part I. Analytical models of twist drill temperature distributions International Journal of Machine Tools and Manufacture, 1990 , v 30 , n 2 , p 203 – 215
[19] Agapiou, J. & Stephenson, D. Analytical and experimental studies of drill temperatures Journal of engineering for industry, American Society of Mechanical Engineers, 1994 , v 116 , n 1 , p 54-60
[20] Bono, M. Thesis on experimental and analytical issues in drilling, The University of Michigan, 2001
[21] Soriano, J. M.; Garay, A.; Aristimuno, P.; Iriarte, L. M.; Eguren, J. A. & Arrazola, P. J. Efects of Rotational Speed, Feed Rate and Tool Type on Temperatures and Cutting Forces when drilling Bovine Cortical Bone Machining Science and Technology, Taylor & Francis, 2013 , v 17 , n 4 , p 611-636
[22] Yan, S.; Zhu, D.; Zhuang, K.; Zhang, X. & Ding, H. Modeling and analysis of coated tool temperature variation in dry milling of Inconel 718 turbine blade considering flank wear effect Journal of Materials Processing Technology, 2014 , v 214 , n 12 , p 2985 – 3001
[23] Stephenson, D. A. & Agapiou, J. S. Metal cutting theory and practice CRC press, 2006 , v 68
[24] Kronenberg, M. Machining science and application: theory and practice for operation and development of machining processes Pergamon Press, 1966
[25] Rech, J.; Arrazola, P.; Claudin, C.; Courbon, C.; Pusavec, F. & Kopac, J. Characterisation of friction and heat partition coefficients at the tool-work material interface in cutting CIRP Annals - Manufacturing Technology, 2013 , v 62 , n 1 , p 79 – 82
[26] Childs, T. Metal machining: theory and applications Hodder Arnold, 2000
[27] Fleischer, J.; Pabst, R. & Kelemen, S. Heat flow simulation for dry machining of power train castings CIRP Annals - Manufacturing Technology, 2007 , v 56 , n 1 , p 117 – 122
[28] Segurajauregui, U. & Arrazola, P. J. Heat-flow determination through inverse identification in drilling of aluminium workpieces with MQL Production Engineering, 2015
[29] Biermann, D. & Iovkov, I. Investigations on the thermal workpiece distortion in MQL deep hole drilling of an aluminium cast alloy CIRP Annals - Manufacturing Technology, 2015 , v 64 , n 1 , p 85 – 88
[30] Solter, J. & Gulpak, M. Heat partitioning in dry milling of steel CIRP Annals - Manufacturing Technology, 2012 , v 61 , n 1 , p 87 - 90
[31] Davies, M.; Ueda, T.; M'saoubi, R.; Mullany, B. & Cooke, A. On the measurement of temperature in material removal processes CIRP Annals-Manufacturing Technology, Elsevier, 2007 , v 56 , n 2 , p 581-604
[32] Brinksmeier, E.; Pecat, O. & Rentsch, R. Quantitative analysis of chip extraction in drilling of Ti6Al4V CIRP Annals - Manufacturing Technology, 2015 , v 64 , n 1 , p 93 - 96
[33] Kwong, J. Thesis on understanding the mechanisms affecting surface integrity during hole making operations on an advanced Ni-based superalloy, The University of Nottingham, 2009
[34] Beno, T. & Hulling, U. Measurement of cutting edge temperature in drilling Procedia CIRP, 2012 , v 3 , n 1 , p 531 – 536
[35] Okada, M.; Ueda, T.; Hosokawa, A. & Tanaka, R. Drilling of difficult-to-cut materials by using indexable insert drill with non-axisymmetrical geometry Nihon Kikai Gakkai Ronbunshu, C Hen/Transactions of the Japan Society of Mechanical Engineers, Part C, 2012 , v 78 , n 785 , p 252 – 261
[36] M'Saoubi, R.; Axinte, D.; Herbert, C.; Hardy, M. & Salmon, P. Surface integrity of nickel-based alloys subjected to severe plastic deformation by abusive drilling CIRP Annals-Manufacturing Technology, Elsevier, 2014 , v 63 , n 1 , p 61-64
[37] Soler, D.; Childs, T. H. & Arrazola, P. J. A Note on Interpreting Tool Temperature Measurements from Thermography Machining Science and Technology, Taylor & Francis, 2015 , v 19 , n 1 , p 174-181

Highlights

- Assessment of the heat fraction to the workpiece (β) when drilling Inconel 718
- Introduction of a model based on a new experimental method (that allows lubricated drilling).
- β values range from 0.23 to 0.065 depending on the cutting and cooling conditions.
- β relative to Peclet show different trends for dry or lubricated conditions.